

Tetrahydroisoquinoline Derivatives As Highly Selective and Potent Rho Kinase Inhibitors

Xingang Fang,[†] Yan Yin,[†] Yen Ting Chen,[†] Lei Yao,[†] Bo Wang,[†] Michael D. Cameron,[†] Li Lin,[†] Susan Khan,[†] Claudia Ruiz,[†] Thomas Schröter,[†] Wayne Grant,[†] Amiee Weiser, Jennifer Pocas,[†] Alok Pachori,[†] Stephan Schürer,[‡] Philip LoGrasso,^{*,†} and Yangbo Feng^{*,†}

[†]Translational Research Institute and Department of Molecular Therapeutics, The Scripps Research Institute, Florida, 130 Scripps Way, 2A1, Jupiter, Florida 33458, and [‡]Department of Pharmacology and Center for Computational Science, University of Miami, Miami, Florida 33136

Received May 11, 2010

Rho kinase (ROCK) is a promising drug target for the treatment of many diseases including hypertension, multiple sclerosis, cancer, and glaucoma. The structure–activity relationships (SAR) around a series of tetrahydroisoquinolines were evaluated utilizing biochemical and cell-based assays to measure ROCK inhibition. These novel ROCK inhibitors possess high potency, high selectivity, and appropriate pharmacokinetic properties for glaucoma applications. The lead compound, **35**, had subnanomolar potency in enzyme ROCK-II assays as well as excellent cell-based potency ($IC_{50} = 51$ nM). In a kinase panel profiling, **35** had an off-target hit rate of only 1.6% against 442 kinases. Pharmacology studies showed that compound **35** was efficacious in reducing intraocular pressure (IOP) in rats with reasonably long duration of action. These results suggest that compound **35** may serve as a promising agent for further development in the treatment of glaucoma.

Introduction

ROCK^a is a protein serine/threonine kinase of ~160 kDa where the kinase domain is located at the N-terminus followed by the coiled-coil domain, the Rho-binding domain, and the pleckstrin homology (PH) domain with an internal cysteine-rich region/domain (CRD) at the C-terminus.¹ ROCK belongs to the AGC kinase family and is most homologous to myotonic dystrophy kinase (DMPK), DMPK-related cell division control protein 42 (Cdc42)-binding kinases (MRCK), and citron kinase (CRIK), and is also closely related to protein kinase A (PKA) and protein kinase B (Akt). ROCK is auto-inhibited in its free form and is activated by association with the GTP-binding form of RhoA. There are two isoforms of ROCK: ROCK-I (ROK β or p160ROCK) and ROCK-II (ROK α), which share 65% identity overall and 92% of identity in the kinase domain. Both ROCK-II and ROCK-I are widely expressed in several tissues but ROCK-II is more abundant in brain tissue.¹

ROCK plays a pivotal role in stress fiber formation,² focal adhesion,² smooth muscle contraction,³ and regeneration of nerve fibers.⁴ Therefore, ROCK inhibitors have potential for the treatment of myocardial ischemia,⁵ hypertension,^{3,6,7} erectile dysfunction,⁸ glaucoma,⁹ cancer migration,^{10,11} spinal-cord injury,¹² multiple sclerosis,¹³ and inflammatory disorders.¹⁴ Fasudil,¹⁵ the only approved ROCK inhibitor, has been marketed as a treatment for cerebral vasospasm in Japan since 1995. Encouraged by the success of Fasudil, various classes of

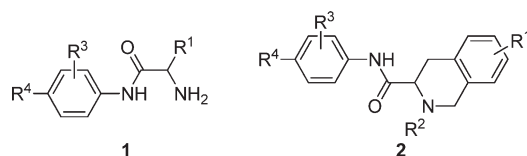


Figure 1. General structures of α -amino anilides.

ROCK inhibitors have been reported including isoquinolines,^{16,17} pyridines (the Y series),³ aminofurazans,¹⁸ dihydropyrimidines,¹⁹ indazoles,²⁰ and azaindoles.²¹ For a recent review, see LoGrasso and Feng 2009.¹⁴ Our group has recently reported potent and selective ROCK inhibitors based on benzodioxane amides,²² chromane amides,²³ benzimidazoles/benzoxazoles,²⁴ benzothiazoles,²⁵ and aniline-ureas.²⁶

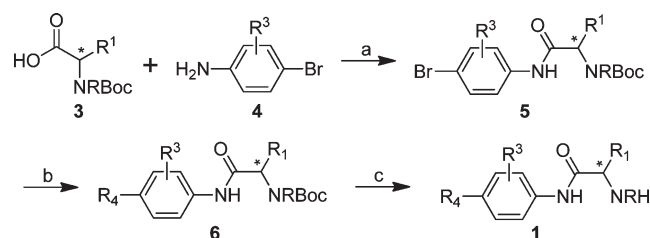
Amino acids are common building blocks in medicinal chemistry. Because of the ready availability of chiral α -amino acids, optically pure compounds can quickly be accessed. In this study, the identification of a new class of potent and selective α -amino anilide-based ROCK inhibitors with general structures **1** and **2** (Figure 1) are reported, and the optimization for structure **2** is described. This class of compounds consisted of a heterocycle that bound to the hinge site in the ROCK-II ATP binding pocket as determined by molecular modeling, an aromatic ring in the middle as a spacer, and an amino acid based amide moiety that is expected to bind to the hydrophobic region under the P-loop in the enzyme. The major findings from this class of compounds include: potent enzyme inhibition of ROCK ($IC_{50} < 1$ nM), potent cell-based activity ($IC_{50}s = 10$ – 50 nM), low oral bioavailability to prevent systemic exposure after topical application, and IOP-lowering ability with long duration of action.

Chemistry

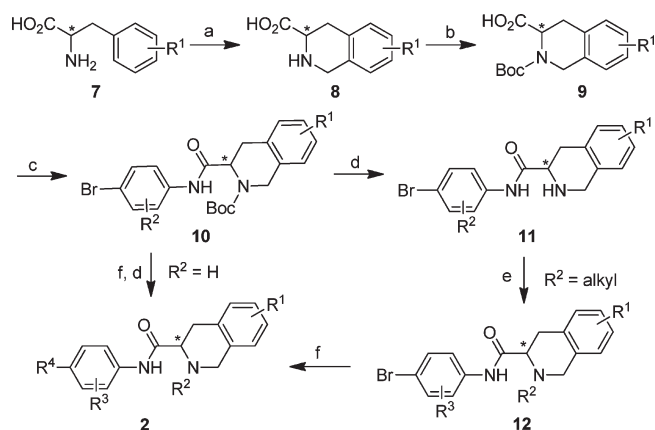
For compounds based on commercially available amino acids (phenylalanines, phenylglycines, and unsubstituted

*To whom correspondence should be addressed. For Y.F.: phone, 561-228-2201; Fax, 561-228-3089; E-mail, yfeng@scripps.edu. For P.L.: phone, 561-228-2230; E-mail, lograsso@scripps.edu.

^aAbbreviations: AUC, pharmacokinetic area under curve; Cl, pharmacokinetic clearance; C_{max} , pharmacokinetic maximum concentration; V_d , volume of distribution; F , oral bioavailability; HLMS, human liver microsomal stability; HTS, high-throughput screening; ppMLC, bisphospho myosin light chain; IOP, intraocular pressure; ROCK, Rho kinase; aqd, once daily.

Scheme 1. General Synthesis of α -Amino Anilides **1**^a

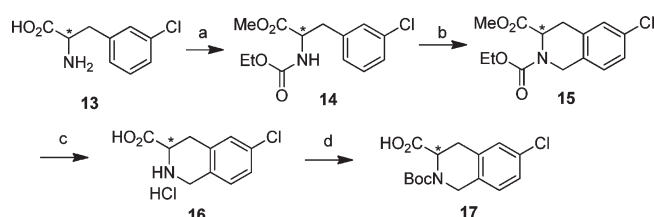
^a Reaction and conditions: (a) HATU, DIPEA, DMF, rt (or 40 °C), 2 h; (b) R⁴ boronic acid or its pinacol ester, Pd(PPh₃)₄, dioxane/water, 140 °C, 30 min, microwave; (c) 1:2 TFA/CH₂Cl₂, triisopropylsilane.

Scheme 2. General Synthesis of 1,2,3,4-Tetrahydroisoquinoline-Based Compounds **2**^a

^a Reaction conditions: (a) 37% formaldehyde in water, 3–6 M HCl solution, 12 h; (b) (Boc)₂O, 1N NaOH, 12 h; (c) HATU, DIPEA, 4-bromoaniline **4**, DMF, rt (or 40 °C), 2 h; (d) TFA/CH₂Cl₂, triisopropylsilane, 1 h; (e) R² aldehyde, NaBH(OAc)₃, CH₂Cl₂, rt, 14 h, then NaBH₄; (f) R⁴ boronic acid pinacol ester, Pd(PPh₃)₄, dioxane/water, 140 °C, 30 min, microwave.

1,2,3,4-tetrahydroisoquinoline-3-carboxylic acids), the typical synthesis of the α -amino anilides with general structure **1** is outlined in Scheme 1. The Boc protected α -amino acid **3** (commercial or obtained in one step from α -amino acids) was condensed with various 4-bromoaniline **4** using HATU as the coupling reagent to provide intermediate **5**, which was then coupled with 1*H*-4-pyrazoleboronic acid pinacol ester under Suzuki conditions to provide amide **6**. Deprotection of Boc group using TFA/CH₂Cl₂ in the presence of 5% triisopropylsilane (TIS) as the scavenger gave the final compound **1**, which was purified by preparative HPLC.

The preparation of structure **2** is summarized in Scheme 2. The Boc protected 1,2,3,4-tetrahydroisoquinoline-3-carboxylic acid **9** was synthesized from phenylalanine **7** by a Pictet–Spengler step with aqueous formaldehyde in an acidic medium followed by the Boc protection of the secondary amino group. The resulting Boc protected tetrahydroisoquinoline **9** was coupled with 4-bromoaniline **4** to form the amide **10**. Suzuki coupling of **10** with the corresponding boronic acid pinacol ester followed by deprotection of the Boc group provided compound **2** containing a free N–H group on tetrahydroisoquinoline moiety. The *N*-alkylated analogue **2** was synthesized by deprotection of the Boc on intermediate **10**, reductive amination²⁷ of **11** with an aldehyde, and Suzuki coupling with the corresponding boronic acid pinacol ester to furnish the final compound **2**. The optical purity (both *R* and

Scheme 3. Synthesis of *N*-Boc-6-chloro-1,2,3,4-tetrahydroisoquinoline-3-carboxylic acid **17**^a

^a Reaction conditions: (a) (i) SOCl₂, MeOH, (ii) EtOCOCl, Et₃N; (b) 3:1 AcOH/H₂SO₄, 4 equiv paraformaldehyde, 10 h; (c) 6 M HCl, reflux, 16 h; (d) (Boc)₂O, 1 M NaOH, 1 h.

S enantiomers) of either **9** or **10** was confirmed by NMR analysis of the corresponding Mosher amides.

Because of insufficient reactivity of the unprotected 3-chlorophenylalanine, an electron withdrawing group *N*-ethoxycarbonyl was applied to provide extra reactivity in the Pictet–Spengler condensation²⁸ in the synthesis of 6-chloro-1,2,3,4-tetrahydroisoquinoline-3-carboxylic acid (Scheme 3). Thus, amino acid **13** was protected as an ester and an ethyl carbamide in two steps to provide intermediate **14**. Compound **14** underwent Pictet–Spengler reaction with paraformaldehyde in a mixture of acetic acid and sulfuric acid (3:1 by volume) to provide the protected 6-chloro-1,2,3,4-tetrahydroisoquinoline **15**. Both the ester and the carbamide groups of **15** were cleaved by refluxing in 6 M HCl. The Boc protection of the amino group furnished intermediate **17**.

Results and Discussion

Our initial literature-based structure design and in-house high-throughput screening²⁹ led to the identification of amide **18** (Figure 2), an α -amino acid amide phenyl-pyrazole structure, as an early lead. Compared to the well-studied (*R*)-4-(1-aminoethyl)-*N*-(pyridin-4-yl)cyclohexanecarboxamide (Y-27632, one of the best Y series compounds) and Fasudil, this compound (Table 1) had higher affinity for ROCK-II (IC₅₀ = 12 nM) as well as good human microsomal stability (*T*_{1/2} = 67 min), although it had moderate potency in cell-based myosin light chain bis-phosphorylation assays (ppMLC)³⁰ (IC₅₀ = 713 nM) and low selectivity against PKA (chosen as routine kinase counter screen because it is closely related to ROCK) (IC₅₀ = 41 nM, 3.4-fold). Our optimization started by replacing the 3-fluorophenylalanine moiety in **18** with a couple of other phenylalanine and phenylglycine-based structures. As shown in Table 1, the 4-chlorophenylalanine-based anilide **19** had higher ROCK-II potency (IC₅₀ = 2 nM) and much improved cell potency (IC₅₀ = 18 nM), but the PKA selectivity still remained low (IC₅₀ = 7 nM, 3-fold). Replacement of the 4-chlorophenylalanine moiety with 4-chlorophenylglycine gave the potent amide **20** (IC₅₀ = 1 nM) with excellent cell activities (IC₅₀ = 25 nM) as well as improved PKA selectivity (IC₅₀ = 23 nM, 23-fold). These results were encouraging but the PKA selectivity for these ROCK inhibitors still needed improvement.

The introduction of a 2-(*N,N*-dimethylamino)ethoxy side chain onto the central phenyl ring (compound **21**, IC₅₀ = 22 nM for ROCK-II) was discovered to be an efficient way to improve the inhibitor's selectivity against PKA (IC₅₀ = 2524 nM, > 100-fold). This change in PKA selectivity was likely due to a much reduced PKA activity. The 2-(*N,N*-dimethylamino)-ethoxy side chain bound to residue Asp176 in the ROCK-II binding pocket (based on our docking pose). The space around

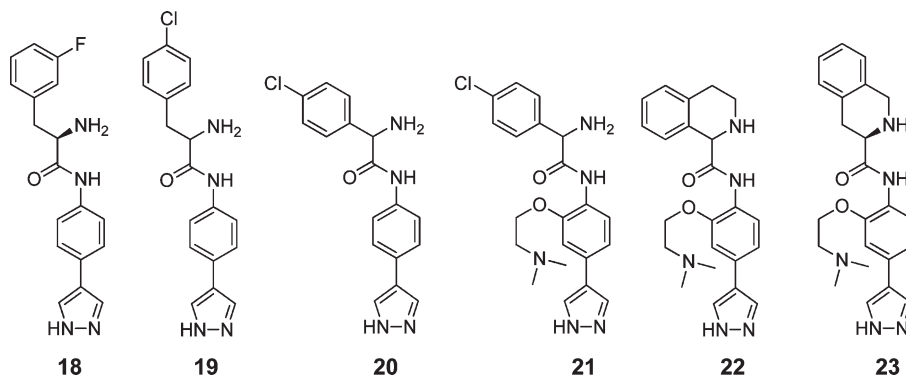


Figure 2. SAR evolution and identification of novel tetrahydroisoquinoline-based ROCK inhibitors.

Table 1. Assay Data for Compounds 18–23

compd	IC ₅₀ ^a (nM)		selectivity (ROCK-II over PKA)	ppMLC cell assay IC ₅₀ ^a (nM)	T _{1/2} (min) ^b HLM
	ROCK-II	PKA			
18	12	41	3.4	713	67
19	2	7	3.5	18	67
20	1	23	23	25	84
21	22	2524	115	310	14
22	371	> 20000	> 54	> 2700	14
23	7	2514	359	32	98

^a Average of two or more experiments and deviation less than 50%.

^b 2 mg/mL human liver microsome (HLM) was employed.

this area of the ATP binding pocket is larger in ROCK than in PKA (the corresponding residue is Glu127 in PKA),^{31,32} and therefore, a large side chain was more tolerated in ROCK. To further improve the PKA selectivity, the bicyclic phenylglycine-based 1,2,3,4-tetrahydroisoquinoline-1-carboxamide **22** was synthesized and evaluated. As shown in Table 1, compound **22** exhibited good selectivity against PKA (> 54-fold) but its ROCK potency was much reduced (IC₅₀ = 371 nM). On the other hand, the bicyclic analogue of the phenylalanine-based compound, 1,2,3,4-tetrahydroisoquinoline-3-carboxamide **23** exhibited excellent selectivity against PKA (IC₅₀ = 2510 nM, 360-fold) as well as high ROCK potency in both enzyme and cell-based assays (IC₅₀ = 7 and 32 nM, respectively), and high microsomal stability (T_{1/2} = 98 min). As a result, all subsequent optimizations were focused on analogues containing the 1,2,3,4-tetrahydroisoquinoline-3-carboxamide moiety.

To gain a better understanding of how our inhibitors bind in the kinase domain of ROCK-II, and more importantly, to direct our optimization strategy, compound **23** was docked into a human ROCK-II model using the method previously described.²² The binding pose illustrated in Figure 3 demonstrated that several key interactions are responsible for the high potency and selectivity of compound **23**. The pyrazole forms a typical 2-hydrogen bond interaction pattern with the kinase hinge residues. The amide carbonyl group of **23** formed a third hydrogen bond with the side chain NH on residue Lys121 in the phosphate binding region. The last important hydrogen bonding element was found between the tertiary amine on the dimethylaminoethoxy side chain of **23** with the carboxylate side chain of Asp176, which explains the high selectivity of **23** compared to those compounds without a side chain on the central phenyl ring. In addition, the pose of compound **23** indicated a hydrophobic interaction in which the aromatic ring of the tetrahydroisoquinoline moiety is immersed into a hydrophobic region under the flexible P-loop

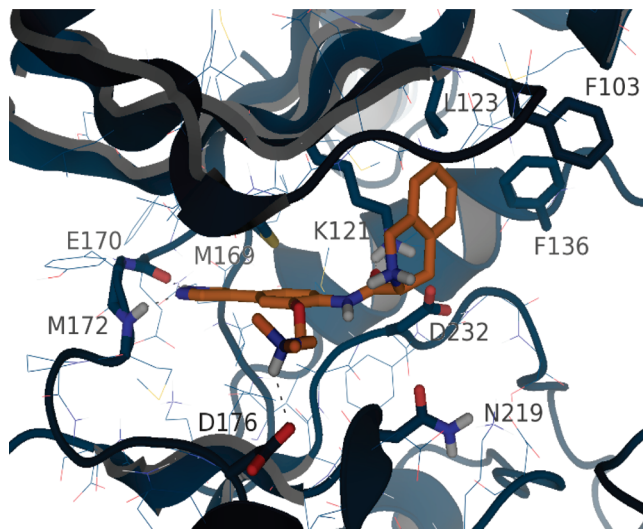
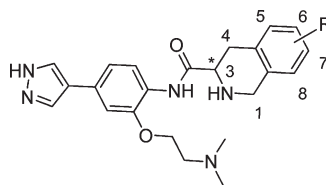


Figure 3. Compound **23** docked into the ROCK-II ATP-binding pocket. H-bonds are shown by dashed lines.

characterized by residues Phe103, Ala102, Leu123, and Phe136. As suggested in our previous studies, this hydrophobic interaction is a major contributor to the high potency of ROCK inhibitors.²²

On the basis of this model, substitutions with reasonable size are expected to be tolerated on the 5- and 6-position of the tetrahydroisoquinoline phenyl ring (Figure 3). Thus, substitution with both electron-donating (methoxy and ethoxy) and electron-withdrawing (F, Cl) groups at the 6-position of the tetrahydroisoquinoline ring was investigated. The 3-position chirality effect of the tetrahydroisoquinoline moiety was first studied. As demonstrated in Table 2, among the four pairs of enantiomers, the unsubstituted (**23**, **24**) and the 6-methoxy substitution (**29**, **30**) favored the *R* configuration while the 6-fluoro substitution (**25**, **26**) favored the *S* configuration. On the other hand, no clear chirality effect was observed for the 6-chloro-substituted ROCK inhibitors (**27**, **28**). The relative configurations of *R* and *S* compounds were confirmed by comparing the ¹H NMR chemical shifts and split patterns of certain hydrogen nuclei on their corresponding Mosher amides,³³ and the results suggested the agreement of the assignment on all 6-OMe, 6-Cl, and 6-F compounds.

Our data (Table 2) indicated that the *R* configured tetrahydroisoquinolines intrinsically bind better to Rho kinase as is the case in isomers **23** vs **24**, and **29** vs **30**. The reversal of the activity trend of the *R* and *S* enantiomers (Table 2) in **25** vs **26** suggests that the 6-F substitution resulted in modulation of

Table 2. SAR Studies on the 1,2,3,4-Tetrahydroisoquinoline Moiety

compd	R	chirality ^c	IC ₅₀ ^a (nM)		selectivity (ROCK-II over PKA)	ppMLC cell assay IC ₅₀ ^a (nM)	T _{1/2} (min) ^b HLM
			ROCK-II	PKA			
23	H	<i>R</i>	7	2514	359	32	98
24	H	<i>S</i>	59	4040	68	868	nd ^d
25	6-F	<i>R</i>	290	6860	24	nd ^d	nd ^d
26	6-F	<i>S</i>	7	3950	564	52	121
27	6-Cl	<i>R</i>	23	4435	193	85	17
28	6-Cl	<i>S</i>	51	11540	226	nd ^d	nd ^d
29	6-OMe	<i>R</i>	10	> 20000	> 2000	41	101
30	6-OMe	<i>S</i>	156	> 20000	> 128	nd ^d	nd ^d
31	6-OEt	<i>Racemate</i>	850	4300	5	nd ^d	nd ^d
32	7-OMe	<i>R</i>	261	> 20000	> 77	nd ^d	nd ^d
33	8-OMe	<i>Racemate</i>	334	> 20000	> 60	nd ^d	nd ^d

^a Average of two or more experiments, and deviation less than 50%. ^b 2 mg/mL human liver microsome was employed. ^c Chirality came from starting material and was confirmed by NMR analysis of the corresponding Mosher amide. ^d Not determined.

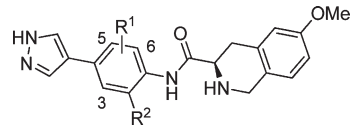
the interactions of the inhibitor distinct from the 6-OMe or unsubstituted tetrahydroisoquinoline derivatives. Different types of interactions between fluorine atoms with protein functional groups have been reported, and in many cases compounds with fluorine substitution behave differently in protein environments compared to similar compounds with different or even other halogen substituents.³⁴ Such fluorine interactions include F–H hydrogen bonds, π -interactions with aromatic or guanidine groups, multipolar interactions, and/or F–nitrogen interactions (halogen bonding).³⁴ These special F-interactions (or the general halogen-interactions) could result in a change of the orientation of the tetrahydroisoquinoline ring under the P-loop. Indeed, this kind of halogen bonding has been shown to be important for 1-aryl-3,4-dihydroisoquinoline inhibitors of JNK3, suggesting this observation does impart potency enhancing elements to kinase inhibitors.³⁵ Because of the direct F-bonding or indirect F-substitution effects, the *S* configuration is preferred for the 6-F tetrahydroisoquinoline-based compounds. In the case of 6-Cl compounds, no clear preference was observed between the *R* and *S* configurations (IC₅₀ is 23 nM vs 51 nM), probably because the halogen-bonding effect of Cl³⁵ is not as significant as that of the F atom.

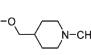
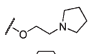
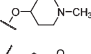
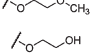
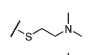
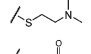
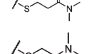
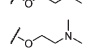
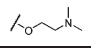
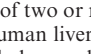
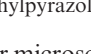
Results in Table 2 demonstrated that, when the preferred enantiomer was applied (i.e., “*R*” in 6-OMe-tetrahydroisoquinoline and “*S*” in 6-F-tetrahydroisoquinoline; compounds **29** and **26**, respectively), small substitutions did not change the inhibitor’s ROCK-II affinity much as compared to the non-substituted compound **23**. On the other hand, a more significant change in ROCK-II activity was observed when the less preferred enantiomer was used (“*S*” in 6-OMe-tetrahydroisoquinoline and “*R*” in 6-F-tetrahydroisoquinoline; compounds **30** and **25**, respectively). Moreover, a larger substitution such as an ethoxy group (compound **31**) significantly reduced the ROCK-II potency. In terms of selectivity against PKA, when the preferred enantiomer was applied, both fluoro (**26**, 564-fold) and methoxy (**29**, > 2000-fold) substitutions were favored as compared to the nonsubstituted **23** (359-fold). However, the large ethoxy substitution (**31**) notably decreased this PKA selectivity (5-fold) apparently due to reduced

ROCK-II potency. This conclusion was also true even when comparing the less preferred enantiomers of tetrahydroisoquinolines whose derivatives contain smaller group substituents (compounds **24**, **25**, and **30**; PKA selectivity was 68, 24, and > 128-fold, respectively). These results suggested that bulky groups at the 6-position of the tetrahydroisoquinoline ring were not as well tolerated in the ROCK-II binding pocket as they were in the corresponding region of the PKA binding pocket. Thus, smaller substitution such as H, F, and OMe were favored for both potency and PKA selectivity when the preferred chirality of the tetrahydroisoquinoline ring was applied. The methoxy group was then applied to different positions of the phenyl ring in the tetrahydroisoquinoline moiety. Results in Table 2 showed that substitutions at the 6-position (**29**) were well tolerated, while substitutions at the 7- and 8-position (**32** and **33**) reduced the ROCK potency. These SAR results are consistent with our docking pose shown in Figure 3, which demonstrated that there was not much room around the 7- and 8-positions of the tetrahydroisoquinoline ring to incorporate a methoxy group.

As described above, the side chain on the central phenyl ring is critical to the inhibitor’s selectivity against PKA (and to some extent, to the high potency of our ROCK inhibitors). To gain a better understanding on how different side chains from several different classes on the central phenyl ring *ortho*- to the amide group were introduced to the 6-methoxy-1,2,3,4-tetrahydroisoquinoline pyrazole compounds. Large *meta*-substitutions were not investigated in this study because they are not well-tolerated as illustrated in our previous study with a different chemotype.¹⁴ As summarized in Table 3, both the potency and PKA selectivity for many of those compounds with a substitution on the central phenyl ring *ortho*- to the aniline amide group were much improved compared to the unsubstituted compound **34**. We believe that the extra binding of the side chain with residue Asp176 in the ROCK-II enzyme is the basis of this effect.

Compounds **35**, **36**, and **37**, which had a tertiary amine containing alkoxy side chain, were potent in both enzymatic and cell-based assays, selective against PKA, and stable in

Table 3. Substitution Effect on the Central Phenyl Ring


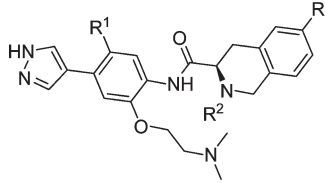
Cmpd	R ¹	R ²	IC ₅₀ ^a (nM)		Selectivity (ROCK-II over PKA)	ppMLC cell assay IC ₅₀ ^a (nM)	T _{1/2} (min) ^b HLM
			ROCK-II	PKA			
34	H	H	134	1680	13	nd ^c	nd ^c
35	H		< 1	5130	> 5130	51	61
36	H		6	>20000	> 3333	218	63
37	H		3	170	57	70	104
38	H		25	9320	373	339	43
39	H		42	5000	119	2700	nd ^c
40	H		15	4190	279	260	22
41 ^d	H		17	3870	228	74	11
42	H		4	1400	350	1786	3
43	3-F		28	>20000	714	250	72
44	5-F		3	>20000	6667	14	51
45	6-F		23	>20000	870	190	112


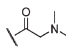
^a Average of two or more experiments, and deviation less than 50%.
^b 2 mg/mL human liver microsomes were employed. ^c Not determined.
^d With 3-methylpyrazol-4-yl as the hinge binding moiety.

human liver microsomes. Among them, compound **35**, which had an (*N*-methyl-piperidin-4-yl)methoxy side chain, was the best overall with subnanomolar (IC₅₀ < 1 nM) ROCK-II potency, high PKA selectivity (> 5000 fold), good cell potency (IC₅₀ = 51 nM) as well as good microsomal stability. The similar compound **37**, which has one less methylene group, was slightly less potent but the PKA selectivity was only 57-fold. Compound **36**, which possesses a 2-(pyrrolidin-1-yl)ethoxy side chain, was also very potent, selective, and stable in human microsomes. Compounds **38** and **39**, which had an ether or a hydroxyl containing alkoxy side chain, were slightly less potent against ROCK-II but still selective over PKA. However, their cell potency was not satisfactory. The tertiary amine containing thioether side chain analogues (compounds **40**, **41**, **42**) were also potent and selective against PKA, yet all these compounds showed low microsomal stability, which might be a result of the easy oxidation of the thioether to sulfone or sulfoxide (observed under acidic condition). The dimethyl amide moiety on compound **42** was even less stable potentially due to demethylation.

After the investigation of monosubstitution on the central phenyl ring, compounds with multiple substitutions (**43**, **44**, and **45**) were also studied. Extra fluoro substitution was introduced on different positions due to the unique role of fluorine in medicinal chemistry.^{36,37} As shown in Table 3, among the three possible substitutions, the 5-F analogue **44** was the best in terms of both enzyme and cell-based potency. However, compared to the nonfluoro substituted compound **29**, compound **44** showed reduced microsomal stability (51 min vs 101 min in **29**) although it had slightly improved potency.

The NH group on the tetrahydroisoquinoline moiety might be a concern because it could harm the compound's capability for membrane penetration such as cornea penetration (an important property for the topical antiglaucoma application).

Table 4. Effects of Fluorination on the Central Ring and Alkylation of the 1,2,3,4-Tetrahydroisoquinoline


Cmpd	R ¹	R ²	R ³	IC ₅₀ ^a (nM)		Selectivity (ROCK-II over PKA)	ppMLC cell assay IC ₅₀ ^a (nM)	T _{1/2} (min) ^b HLM
				ROCK-II	PKA			
23	H	H	H	7	2510	359	32	98
46	F	H	H	6	4710	785	15	45
47	F	Me	H	18	11100	617	62	16
48	F	Et	H	2	13100	6550	11	1
49	F		H	29	>20000	> 690	18	3
50	F		H	775	>20000	> 26	nd ^c	14
29	H	H	OMe	10	>20000	> 2000	41	101
51	H	Et	OMe	9	14430	1603	32	11

^a Average of two or more experiments, and deviation less than 50%.
^b 2 mg/mL human liver microsomes were employed. ^c Not determined.

Thus, N-substitution on this group was investigated (Table 4) because our modeling pose shown in Figure 3 suggested that a substitution on the NH might be tolerated. Results in Table 4 demonstrated that *N*-ethyl (compounds **48** and **51**) and *N*-cyclopropylmethyl (compound **49**) substitutions led to improved selectivity against PKA, while the methyl group (**47**) slightly reduced the potency and PKA selectivity. On the other hand, *N*-acylation of NH produced a compound (**50**) with low ROCK-II activity (IC₅₀ = 775 nM). This is probably because the amide carbonyl group is a strong H-bond acceptor, resulting in negative modulation of the enzyme–ligand interactions. It is also noteworthy that all these N-substituted compounds had much reduced human microsomal stabilities as compared to those free amino compounds **23**, **29**, and **46**, probably due to the dealkylation of tertiary amines.

To examine the selectivity profile of our tetrahydroisoquinoline-based ROCK inhibitors, compounds **29**, **35**, **46**, and **48** were selected for counter screening against several protein kinases other than PKA. As summarized in Table 5, these compounds were generally inactive against JNK3 and p38. The selectivity against MRCKα (belongs to the same kinase family as ROCK) was lower but still reasonable (> 55-fold). Examination of ROCK-I activities indicated that these compounds were pan-ROCK inhibitors. Inhibition of a few cytochrome P450 isoforms, 1A2, 2C9, 2D6, and 3A4, was also studied and single-dose P450 results suggested that P450 inhibition was not an issue for these compounds with the highest inhibition being ~80% at 10 μM for **46** (CYP2D6) and ~70% for **48** (CYP2C9) (Table 5). Data for CYP3A4, the isoform of highest concern, showed all compounds were clean.

To further investigate the general selectivity of these tetrahydroisoquinoline-based ROCK inhibitors, compound **35** was selected to be profiled against a large panel of kinases. Single point profiling of 442 kinases (Ambit Screen³⁸) at 3 μM (a concentration more than 3000-fold of its ROCK-II IC₅₀ value of < 1 nM, Table 3) identified only seven other kinases whereby **35** showed > 65% inhibition: Clk1(86%), Clk4

Table 5. Selectivity of the Lead Compounds over Other Kinases and Cytochrome P450 Isoforms

compd	% inh at 10 μ M 1A2/2C9/2D6/3A4	IC ₅₀ (nM) ^a				
		ROCK-II	ROCK-I	MRCK α	JNK3	p38
46	31/62/77/18	6	33	333	> 20000	> 20000
29	21/31/40/-3	10	48	5350	> 20000	> 20000
35	3/45/52/15	< 1	10	669	> 20000	> 20000
48	-24/70/52/39	2	16	810	> 20000	> 20000

^a Average of two or more experiments, and deviation less than 50%.

Table 6. Rat Pharmacokinetic Data of Selected Compounds^a

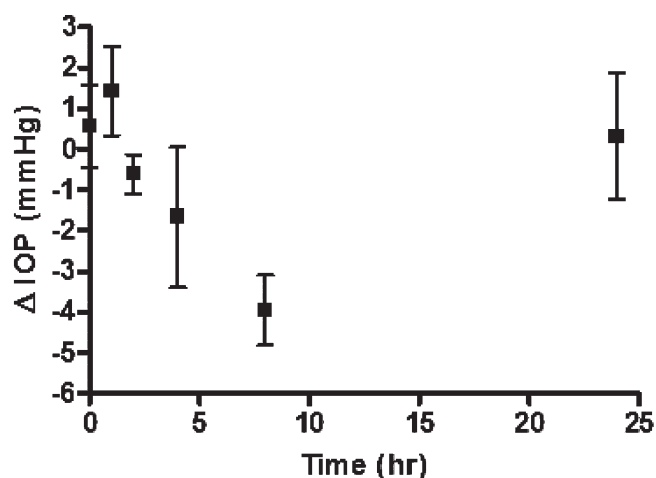
compd	Cl (mL/min/kg)	V _d (L/kg)	t _{1/2} (h)	C _{max} PO (nM)	oral F (%)
29	17	7.2	5.5	242	28
35	41	9.5	3.4	0	0
44	4.6	0.49	1.5	32	0.3
46	106	24	2.7	18	16
49	42	7	2.3	0	0
51	130	17	1.7	0	0

^a Data is the average from three sets dosed at 1.0 mg/kg (iv) or 2.0 mg/kg (PO).

(91%), Lats2 (75%), MRCK β (77%), NDR1 (72%), PI3K β (74%), and STK33 (66%). All other kinases showed either no or very low inhibition (see Supporting Information). An off-target hit rate of only 1.6% (7 out of 442) makes this compound a remarkably selective ATP-competitive kinase inhibitor.³⁸ Multiple interactions between **35** and the enzyme are believed to be the reason for this high general kinase selectivity. In addition to the four interactions observed in the docking pose (Figure 3), two more interactions are highly possible: one is between the tetrahydroisoquinoline NH group and the DFG chain, either directly or through a water molecule; another one is an H-bond between the methoxy group on the tetrahydroisoquinoline ring and the surrounding residues on the enzyme, either directly or via a water molecule. More importantly, all these interactions are believed to be optimal between **35** and ROCK-II, but not other kinases.

The pharmacokinetic properties in rats for compounds **29**, **35**, **44**, **46**, **49**, and **51** were evaluated (Table 6). All tested compounds except **29** and **44** showed high clearance (Cl), high volume of distribution (V_d), low oral C_{max}, and minimal to low bioavailability (F). Compound **44** also had very low oral bioavailability (0.3%). These PK properties are desirable for the topical applications of compounds to be used as antiglaucoma agents, preventing systemic exposure of compound that drains through the tear duct. Because oral exposure of compounds could be achieved through drainage of compounds through the tear duct, and ROCK inhibitors have been shown to reduce blood pressure, PK properties such as low oral bioavailability and high clearance might be beneficial for this class of compounds even when formulated for topical dosing.

The IOP lowering effect of these tetrahydroisoquinoline-based ROCK inhibitors was investigated on the eyes of Brown Norway rats ($n = 7$ /group) housed under constant low-light conditions. Thus, compound **35** was applied at 40 μ g/dose ($2 \times 20 \mu$ L drops of a 0.1% solution) to rat eyes of an elevated IOP model³⁹ (initial IOP was 29 mmHg). As shown in Figure 4, significant decreases in IOP were detected from around 2 h, maximized at or after 8 h, and IOP returning to baseline at 24 h as compared to the vehicle. Data in Figure 4 also indicated that the duration of action for **35** on IOP lowering was long enough to possibly warrant aq dosing regimen even at a concentration of 0.1%. These results demonstrated that tetra-

**Figure 4.** Rat IOP effects of **35** (IOP decreases relative to vehicle).

hydroisoquinoline-based ROCK inhibitors are promising drug candidates as antiglaucoma therapeutics. Future investigation for these compounds will be focused on improved IOP lowering ($\geq 20\%$) at low concentration ($\leq 0.1\%$), ocular stability, ocular pharmacokinetics, and toxicity studies such as the hyperemia effect, which was observed in rabbits and monkeys after long-term dosing of other ROCK compounds.⁴⁰

Conclusion

In this study, we have developed a series of tetrahydroisoquinoline-based amides as ROCK inhibitors starting from the initial lead **18**. SAR investigation and optimization successfully provided potent compounds with high selectivity as well as pharmacokinetic properties that might be desirable for antiglaucoma applications. SAR features attributed to this high potency, selectivity, and low oral bioavailability includes: a tertiary amine containing alkoxy side chain on the central phenyl ring, interactions of the tetrahydroisoquinoline moiety in the hydrophobic pocket of ROCK-II, and methoxy substitution on the tetrahydroisoquinoline. Compound **35**, a highly potent and selective inhibitor with ROCK-II potency in the subnanomolar range and an off-target hit rate of only 1.6% against a panel of 442 kinases, was demonstrated to be effective in reducing intraocular pressure (IOP) on rat eyes. Future optimizations for these tetrahydroisoquinoline-based ROCK inhibitors will be mainly focused on toxicity issues, physicochemical stabilities, and the pharmacokinetic properties that might be dedicated to nontopical administration for other ROCK-related indications. These studies will be reported in due course.

Experimental Section

Chemical Materials and Methods. Proton nuclear magnetic resonance (¹H NMR, ¹³C NMR, ¹⁹F NMR) spectra were recorded at 400 MHz (Bruker), and chemical shifts are reported

in parts per million downfield (δ) from Me_4Si ($\delta = 0.0$). Analytical HPLC data were generated by injecting 10 μL of very dilute sample solution in methanol or acetonitrile to a reverse phase HPLC system run over 14 min (5–95% acetonitrile/water with 0.1% TFA in each solvent). The products were detected by UV in the detection range of 215–310 nm. LC-MS data were collected from Thermo or Agilent instrument. HRMS (electrospray ionization) experiments were performed with a Thermo Finnigan orbitrap mass analyzer. Data were acquired in the positive ion mode at a resolving power of 100000 at m/z 400. Calibration was performed with an external calibration mixture immediately prior to analysis. Final products were all purified by reverse-phase preparative HPLC to provide a purity of > 95% based on UV detection (at 254 nm) in analytical HPLC traces.

General Procedure A: (*R*)-*N*-(4-(1*H*-Pyrazol-4-yl)phenyl)-2-amino-3-(3-fluorophenyl)propanamide (18). To a stirred solution of *N*-Boc protected *D*-3-fluoro-phenylalanine (62 mg, 0.22 mmol) in dry DMF (2 mL) was added 4-bromoaniline (34 mg, 0.2 mmol), DIPEA (0.174 mL, 1.0 mmol), and HATU (91 mg, 0.24 mmol) consequently. The solution was stirred at ambient temperature for 4 h until LC-MS indicated that all aniline was consumed. The reaction mixture was concentrated, and the residue was diluted with EtOAc. The resulting solution was then washed with saturated NaHCO_3 solution and brine and dried over anhydrous Na_2SO_4 . The solvent was evaporated to provide the crude bromo-amide, which was used in the next step without further purification.

The crude amide (0.2 mmol), pyrazole boronic pinacol ester (54 mg, 0.28 mmol), K_2CO_3 (111 mg, 0.8 mmol), and palladium tetrakis(triphenylphosphine) (23 mg, 0.02 mmol) was suspended in 4:1 dioxane/water (2 mL). The resulting mixture was sealed in a microwave tube. The suspension was degassed under vacuum and charged with argon. It was then heated on microwave oven at 140 $^\circ\text{C}$ for 30 min. After the completion of reaction as indicated by LC-MS, the reaction mixture was cooled to room temperature. After concentration, the residue was suspended in EtOAc. The mixture was washed with saturated NaHCO_3 solution and brine. It was filtered and concentrated to provide the crude intermediate, which was treated with 1:1 TFA/ CH_2Cl_2 in the presence of 5% of triisopropylsilane as scavenger. The reaction was stirred at ambient temperature for 30 min to remove the *N*-Boc group. After the solvent was removed under reduced pressure, the residue was subjected to preparative HPLC to provide **18** (24 mg, 37% over 3 steps) as a fine powder of its TFA salt. ^1H NMR ($\text{DMSO}-d_6$, 400 MHz) δ 3.18 (m, 2H), 4.19 (bs, 1H), 7.11 (m, 2H), 7.36 (m, 1H), 7.54 (m, 5H), 8.01 (s, 2H), 8.36 (s, 2H), 10.44 (s, 1H). Single peak in analytical HPLC. LC-MS (ESI): m/z 325 [$\text{M} + 1$] $^+$. HRMS (ESI), MH^+ calcd for $\text{C}_{18}\text{H}_{17}\text{FN}_4\text{O}$, 325.1486; found, 325.1456.

Compounds **18–46** were prepared according to general procedure A:

***N*-(4-(1*H*-Pyrazol-4-yl)phenyl)-2-amino-3-(3-chlorophenyl)propanamide (19).** ^1H NMR ($\text{DMSO}-d_6$, 400 MHz) δ 2.98–3.03 (dd, $J = 7.6, 13.6$ Hz, 1H), 3.08–3.13 (dd, $J = 6.0, 13.6$ Hz, 1H), 4.05–4.06 (m, 1H), 7.21–7.23 (m, 2H), 7.33–7.35 (m, 2H), 7.41–7.44 (m, 2H), 7.51–7.53 (m, 2H), 7.95 (s, 2H), 8.23 (m, 3H), 10.32 (s, 1H). Single peak in analytical HPLC. LC-MS (ESI): m/z 341 [$\text{M} + 1$] $^+$. HRMS (ESI-Orbitrap), MH^+ calcd for $\text{C}_{18}\text{H}_{17}\text{ClN}_4\text{O}$, 341.1191; found, 341.1162.

***N*-(4-(1*H*-Pyrazol-4-yl)phenyl)-2-amino-2-(4-chlorophenyl)acetamide (20).** ^1H NMR ($\text{DMSO}-d_6$, 400 MHz) δ 5.30 (m, 1H), 7.45–7.52 (m, 8H), 7.93 (s, 2H), 8.67 (m, 3H), 10.51 (s, 1H). Single peak in analytical HPLC. LC-MS (ESI): m/z 327 [$\text{M} + 1$] $^+$. HRMS (ESI-Orbitrap), MH^+ calcd for $\text{C}_{17}\text{H}_{15}\text{ClN}_4\text{O}$, 327.1034; found, 327.1005.

2-Amino-2-(4-chlorophenyl)-*N*-(2-(2-(dimethylamino)ethoxy)-4-(1*H*-pyrazol-4-yl)phenyl)acetamide (21). ^1H NMR ($\text{MeOH}-d_4$, 400 MHz), δ 2.86 (s, 6H), 3.59–3.40 (m, 2H), 4.51–4.31 (m, 2H), 5.42 (s, 1H), 7.30–7.24 (m, 2H), 7.64–7.53 (m, 4H), 7.89 (d,

$J = 8.3$ Hz, 1H), 8.01 (s, 2H). Single peak in analytical HPLC. LC-MS (ESI): m/z 414 [$\text{M} + 1$] $^+$. HRMS (ESI-Orbitrap), MH^+ calcd for $\text{C}_{21}\text{H}_{24}\text{ClN}_5\text{O}_2$, 414.1718; found, 414.1689.

***N*-(2-(2-(Dimethylamino)ethoxy)-4-(1*H*-pyrazol-4-yl)phenyl)-1,2,3,4-tetrahydroisoquinoline-1-carboxamide (22).** ^1H NMR ($\text{MeOH}-d_4$, 400 MHz) δ 3.06 (s, 6H), 3.50–3.58 (m, 2H), 3.68–3.79 (m, 2H), 4.52–4.64 (m, 5H), 4.75 (s, 1H), 7.30–7.38 (m, 4H), 7.40–7.44 (m, 2H), 8.06–8.10 (m, 3H). ^{13}C NMR ($\text{CH}_3\text{CN}-d_3$, 100 MHz) δ 31.0, 48.1, 56.9, 57.7, 68.2, 110.7, 119.9, 124.8, 125.3, 127.9, 128.6, 129.0, 129.2, 130.1, 132.6, 150.1, 168.1. Single peak in analytical HPLC. LC-MS (ESI): m/z 406 [$\text{M} + 1$] $^+$. HRMS (ESI-Orbitrap), MH^+ calcd for $\text{C}_{23}\text{H}_{27}\text{N}_5\text{O}_2$, 406.2264; found, 406.2235.

(*R*)-*N*-(2-(2-(Dimethylamino)ethoxy)-4-(1*H*-pyrazol-4-yl)phenyl)-1,2,3,4-tetrahydroisoquinoline-3-carboxamide (23). ^1H NMR ($\text{CH}_3\text{CN}-d_3$, 400 MHz), δ 2.80–2.95 (m, 1H), 3.29–3.39 (m, 1H), 3.48–3.64 (m, 2H), 4.30–4.50 (m, 3H), 4.62 (dd, $J = 11.3, 4.8$ Hz, 1H), 5.73 (bs, 1H), 7.05–7.45 (m, 5H), 7.77–8.29 (m, 2H), 9.54 (bs, 1H), 10.18 (bs, 1H). ^{13}C NMR ($\text{CH}_3\text{CN}-d_3$, 100 MHz) δ 30.6, 45.2, 56.7, 57.4, 63.2, 110.6, 119.5, 124.5, 125.3, 127.6, 128.3, 129.0, 129.1, 129.7, 132.1, 149.9, 167.9. Single peak in analytical HPLC. LC-MS (ESI): m/z 406 [$\text{M} + 1$] $^+$. HRMS (ESI-Orbitrap), MH^+ calcd for $\text{C}_{23}\text{H}_{27}\text{N}_5\text{O}_2$, 406.2264; found, 406.2238.

(*S*)-*N*-(2-(2-(Dimethylamino)ethoxy)-4-(1*H*-pyrazol-4-yl)phenyl)-1,2,3,4-tetrahydroisoquinoline-3-carboxamide (24). ^1H NMR ($\text{CH}_3\text{CN}-d_3$, 400 MHz) δ 2.97–2.88 (b, 1H), 3.36–3.27 (m, 1H), 3.66–3.44 (m, 2H), 4.53–4.31 (m, 3H), 4.62 (dd, $J = 11.27, 4.84$ Hz, 1H), 5.77 (b, 1H), 7.43–7.01 (m, 5H), 8.29–7.77 (m, 2H), 9.66 (bs, 1H), 10.28 (bs, 1H). ^{13}C NMR ($\text{CH}_3\text{CN}-d_3$, 100 MHz) δ 31.0, 45.1, 56.9, 57.7, 63.2, 110.7, 119.9, 124.8, 125.3, 127.9, 128.6, 129.0, 129.2, 130.1, 132.6, 150.1, 168.1. Single peak in analytical HPLC. LC-MS (ESI): m/z 406 [$\text{M} + 1$] $^+$. HRMS (ESI-Orbitrap), MH^+ calcd for $\text{C}_{23}\text{H}_{27}\text{N}_5\text{O}_2$, 406.2264; found, 406.2235.

General Procedure B: (*R*)-*N*-(2-(2-(Dimethylamino)ethoxy)-4-(1*H*-pyrazol-4-yl)phenyl)-6-fluoro-1,2,3,4-tetrahydroisoquinoline-3-carboxamide (25). Aqueous formaldehyde (37%, 1.49 g, 20 mmol) was added to a suspension of *D*-3-fluoro-phenylalanine (930 mg, 5 mmol) in 6 M hydrochloric acid (6 mL). The mixture was stirred at ambient temperature overnight and a white precipitate appeared. The precipitate was filtered off and washed with 1 M HCl solution. The solid was collected and dried under vacuum to provide crude (*R*)-6-fluoro-1,2,3,4-tetrahydroisoquinoline-3-carboxylic acid HCl salt as white solid. This intermediate was then dissolved in 1:1 M NaOH/dioxane (25 mL), and the solution of di-*tert*-butyl dicarbonate (958 mg, 5.5 mmol) in 12 mL of dioxane was added. The mixture was stirred at ambient temperature for 2 h. After the completion of reaction, the reaction mixture was poured into 100 mL of 1 M aqueous citric acid solution, which was extracted three times with EtOAc. The combined organic layer was washed with brine and dried over anhydrous Na_2SO_4 . After filtration, all solvent was evaporated and the residue was subjected to flash chromatography (0–15% of MeOH in CH_2Cl_2) to provide the intermediate (*R*)-2-(*tert*-butoxycarbonyl)-6-fluoro-1,2,3,4-tetrahydroisoquinoline-3-carboxylic acid. General procedure A was then employed to finish the synthesis of **25**. ^1H NMR ($\text{MeOH}-d_4$, 400 MHz) δ 2.99–3.06 (m, 8H), 3.43–3.61 (m, 1H), 3.61–3.79 (m, 2H), 4.41–4.62 (m, 4H), 7.04–7.42 (m, 5H), 7.97–8.05 (m, 3H), 9.87–9.97 (m, 3H), 10.01 (b, 1H). Single peak in analytical HPLC. LC-MS (ESI): m/z 424 [$\text{M} + 1$] $^+$; HRMS (ESI-Orbitrap), MH^+ calcd for $\text{C}_{23}\text{H}_{26}\text{FN}_5\text{O}_2$, 424.2170; found, 424.2141.

The 1,2,3,4-tetrahydroisoquinoline moiety of compounds **26**, **29–31**, and **33–46** were prepared according to general procedure B:

(*S*)-*N*-(2-(2-(Dimethylamino)ethoxy)-4-(1*H*-pyrazol-4-yl)phenyl)-6-fluoro-1,2,3,4-tetrahydroisoquinoline-3-carboxamide (26). ^1H NMR ($\text{MeOH}-d_4$, 400 MHz) δ 2.99–3.03 (m, 2H), 3.05 (s, 6H), 3.43–3.61 (m, 1H), 3.61–3.79 (m, 2H), 4.41–4.48 (m, 1H), 4.51–4.64 (m, 3H), 7.04–7.24 (m, 2H), 7.28–7.42 (m, 3H), 7.99–8.04 (m, 3H), 9.87 (b, 1H), 9.90–9.98 (m, 3H), 10.01 (b, 1H).

Single peak in analytical HPLC. LC-MS (ESI): m/z 424 $[M + 1]^+$. HRMS (ESI-Orbitrap), MH^+ calcd for $C_{23}H_{26}FN_5O_2$, 424.2170; found, 424.2139.

(*R*)-*N*-(2-(2-(Dimethylamino)ethoxy)-4-(1*H*-pyrazol-4-yl)phenyl)-6-chloro-1,2,3,4-tetrahydroisoquinoline-3-carboxamide (27). To 30 mL of anhydrous MeOH was slowly added thionyl chloride (1.5 g, 12.5 mmol) at 0 °C. After stirring for additional 10 min, *D*-3-chloro-phenylalanine (1 g, 5 mmol) was added in several portions. The reaction mixture was then warmed to room temperature and stirred overnight until reaction was complete. The solvent was removed by evaporation, and the residue was diluted with 200 mL of EtOAc. The resulting mixture was washed with saturated $NaHCO_3$ solution, brine, and dried over anhydrous Na_2SO_4 . Filtration followed by concentration provided the crude amino acid methyl ester.

The crude ester was then dissolved in 50 mL of dichloromethane followed by the addition of pyridine (0.809 mL, 10 mmol). The reaction mixture was cooled to 0 °C, and ethyl chloroformate (0.540 mL, 5.5 mmol) was then added carefully. The reaction mixture was warmed to room temperature and stirred overnight until the reaction was complete. Solvent was evaporated, and the residue was diluted with EtOAc. The resulting mixture was washed with 1 M HCl, brine, saturated $NaHCO_3$ solution, and brine consequently, and dried over anhydrous Na_2SO_4 . After filtration and concentration, the residue was dried under vacuum to provide crude (*R*)-6-chloro-2-(ethoxycarbonyl)-1,2,3,4-tetrahydroisoquinoline-3-carboxylic acid, methyl ester (1.17 g, 4.1 mmol), which was used for following transformations.

To the solution of the ester from last step in 3:1 AcOH/sulfuric acid (6 mL), paraformaldehyde (0.135 g, 4.5 mmol) was added. The solution was then stirred overnight to complete the reaction. It was quenched by pouring into 200 mL of ice water. The resulting mixture was extracted with EtOAc three times. The combined organic layer was then washed with saturated $NaHCO_3$ solution, brine, and dried over anhydrous Na_2SO_4 . After filtration and concentration, the crude product was obtained and was directly used in next step.

The intermediate was suspended in 6 M HCl solution and refluxed overnight until ethoxy carbonyl and ester group were completely removed (monitored by LC-MS). The solvents were removed under reduced pressure, and the solid residue was dissolved in 20 mL of 1:1 M NaOH/dioxane to form a solution, to which a solution of di-*tert*-butyl dicarbonate (1.05 g, 4.8 mmol) in 10 mL of dioxane was added slowly. The reaction mixture was stirred for 2 h until the reaction was complete. It was quenched and acidified by pouring into 100 mL of 1 M citric acid solution. The solution was extracted with EtOAc three times, and the combined organic layer was washed with brine and dried over anhydrous Na_2SO_4 . After concentration, flash chromatography was applied (3–10% of MeOH in CH_2Cl_2) to provide the (*R*)-2-(*tert*-butoxycarbonyl)-6-chloro-1,2,3,4-tetrahydroisoquinoline-3-carboxylic acid as pale-yellow syrup. General procedure A was then employed to provide the titled compound. 1H NMR (MeOH- d_4 , 400 MHz) δ 2.76–2.80 (m, 2H), 2.82 (s, 6H), 3.22–3.28 (m, 2H), 3.85–4.10 (m, 5H), 7.32–7.60 (m, 5H), 7.76 (d, J = 6.5 Hz, 1H), 8.50 (s, 2H). Single peak in analytical HPLC. LC-MS (ESI): m/z 440 $[M + 1]^+$.

(*S*)-*N*-(2-(2-(Dimethylamino)ethoxy)-4-(1*H*-pyrazol-4-yl)phenyl)-6-chloro-1,2,3,4-tetrahydroisoquinoline-3-carboxamide (28). The titled compound was synthesized according to the procedures described in the synthesis of compound 27. 1H NMR (MeOH- d_4 , 400 MHz) δ 2.76–2.82 (m, 8H), 3.21–2.25 (m, 2H), 3.89–4.12 (m, 5H), 7.32–7.41 (m, 2H), 7.51–7.60 (m, 3H), 7.73 (d, J = 6.5 Hz, 1H), 8.48 (s, 2H). Single peak in analytical HPLC. LC-MS (ESI): m/z 440 $[M + 1]^+$.

(*R*)-*N*-(2-(2-(Dimethylamino)ethoxy)-4-(1*H*-pyrazol-4-yl)phenyl)-6-methoxy-1,2,3,4-tetrahydroisoquinoline-3-carboxamide (29). 1H NMR (DMSO- d_6 , 400 MHz) δ 2.64–2.75 (m, 1H), 2.86–2.92 (m, 1H), 2.96 (s, 6H), 3.04–3.17 (m, 1H), 3.33 (dd,

J = 17.0, 4.3 Hz, 1H), 3.58 (s, 1H), 3.76 (s, 3H), 3.78–3.87 (m, 1H), 4.25–4.54 (m, 4H), 6.86–7.01 (m, 3H), 7.13–7.40 (m, 4H), 7.73–7.80 (m, 1H), 8.10 (s, 2H). ^{13}C NMR (CH_3CN-d_3 , 100 MHz) δ 34.1, 45.1, 54.8, 56.9, 57.7, 63.2, 110.8, 114.2, 114.9, 119.4, 121.2, 124.0, 125.5, 127.7, 131.1, 134.7, 146.9, 156.2, 167.0. Single peak in analytical HPLC. LC-MS (ESI): m/z 436 $[M + 1]^+$. HRMS (ESI-Orbitrap), MH^+ calcd for $C_{24}H_{29}N_5O_3$, 436.2370; found, 436.2340.

(*S*)-*N*-(2-(2-(Dimethylamino)ethoxy)-4-(1*H*-pyrazol-4-yl)phenyl)-6-methoxy-1,2,3,4-tetrahydroisoquinoline-3-carboxamide (30). 1H NMR (DMSO- d_6 , 400 MHz) δ 2.65–2.74 (m, 1H), 2.82–2.89 (m, 1H), 2.94 (s, 6H), 3.04–3.17 (m, 1H), 3.30–3.35 (m, 1H), 3.59 (m, 1H), 3.74 (s, 3H), 3.77–3.88 (m, 1H), 4.24–4.55 (m, 4H), 6.86 (m, 3H), 7.10–7.39 (m, 4H), 7.70–7.80 (m, 1H), 8.11 (s, 2H). ^{13}C NMR (CH_3CN-d_3 , 100 MHz) δ 34.9, 45.8, 54.9, 57.5, 58.3, 63.2, 111.0, 114.3, 115.2, 119.9, 121.7, 124.4, 126.5, 127.9, 131.5, 135.0, 147.2, 155.9, 168.0. Single peak in analytical HPLC. LC-MS (ESI): m/z 436 $[M + 1]^+$.

N-(2-(2-(Dimethylamino)ethoxy)-4-(1*H*-pyrazol-4-yl)phenyl)-6-ethoxy-1,2,3,4-tetrahydroisoquinoline-3-carboxamide (31). 1H NMR (DMSO- d_6 , 400 MHz) δ 1.36–1.26 (m, 3H), 2.55 (t, J = 5.6 Hz, 2H), 2.89 (s, 6H), 3.16–3.04 (m, 1H), 2H), 3.41–3.32 (m, 1H), 3.67–3.49 (m, 2H), 4.06–3.97 (m, 1H), 4.54–4.24 (m, 4H), 7.02–6.85 (m, 3H), 7.37–7.12 (m, 4H), 7.80–7.75 (m, 1H), 8.16–8.06 (m, 2H). ^{13}C NMR (CH_3CN-d_3 , 100 MHz) δ 29.6, 34.3, 43.6, 56.0, 63.2, 65.0, 109.2, 111.9, 113.7, 114.8, 117.7, 119.5, 121.2, 123.1, 124.1, 127.5, 130.7, 132.2, 148.5, 158.4, 160.0, 166.7. Single peak in analytical HPLC. LC-MS (ESI): m/z 450 $[M + 1]^+$.

(*R*)-*N*-(2-(2-(Dimethylamino)ethoxy)-4-(1*H*-pyrazol-4-yl)phenyl)-7-methoxy-1,2,3,4-tetrahydroisoquinoline-3-carboxamide (32). 1H NMR (DMSO- d_6 , 400 MHz) δ 2.86–2.92 (m, 1H), 2.82 (s, 6H), 3.04–3.17 (m, 1H), 3.27–3.30 (m, 1H), 3.49 (s, 1H), 3.64 (s, 3H), 3.78–3.87 (m, 1H), 4.23–4.38 (m, 2H), 6.71–6.81 (m, 2H), 7.10–7.12 (m, 1H), 7.58–7.37 (d, J = 6.8 Hz, 1H), 7.74–7.80 (m, 2H), 7.99 (s, 2H), 9.49 (b, 1H), 9.59 (b, 1H), 9.82 (m, 2H). Single peak in analytical HPLC. LC-MS (ESI): m/z 436 $[M + 1]^+$. HRMS (ESI-Orbitrap), MH^+ calcd for $C_{24}H_{29}N_5O_3$, 436.2370; found, 436.2340.

N-(2-(2-(Dimethylamino)ethoxy)-4-(1*H*-pyrazol-4-yl)phenyl)-8-methoxy-1,2,3,4-tetrahydroisoquinoline-3-carboxamide (33). 1H NMR (MeOH- d_4 , 400 MHz) δ 2.86–2.92 (m, 1H), 2.99 (s, 6H), 3.04–3.17 (m, 1H), 3.52 (dd, J = 19.0, 4.0 Hz, 1H), 3.67–3.79 (m, 1H), 3.82 (s, 3H), 4.37–4.45 (m, 1H), 4.53–4.62 (m, 3H), 6.88–6.94 (m, 3H), 7.20–7.25 (m, 1H), 7.40–7.44 (m, 1H), 8.05–8.09 (m, 3H). Single peak in analytical HPLC. LC-MS (ESI): m/z 436 $[M + 1]^+$. HRMS (ESI-Orbitrap), MH^+ calcd for $C_{24}H_{29}N_5O_3$, 436.2370; found, 436.2341.

(*R*)-*N*-(4-(1*H*-Pyrazol-4-yl)phenyl)-6-methoxy-1,2,3,4-tetrahydroisoquinoline-3-carboxamide (34). 1H NMR (MeOH- d_4 , 400 MHz) δ 3.29–3.20 (m, 1H), 3.46 (dd, J = 17.0, 4.8 Hz, 1H), 3.79 (s, 3H), 4.28 (dd, J = 12.1, 4.8 Hz, 1H), 4.40 (m, 2H), 6.94–6.81 (m, 2H), 7.17 (d, J = 8.5 Hz, 1H), 7.68–7.53 (m, 4H), 7.98–7.95 (m, 2H). Single peak in analytical HPLC. LC-MS (ESI): m/z 349 $[M + 1]^+$. HRMS (ESI-Orbitrap), MH^+ calcd for $C_{20}H_{20}N_4O_2$, 349.1686; found, 349.1656.

(*R*)-6-Methoxy-*N*-(2-((1-methylpiperidin-4-yl)methoxy)-4-(1*H*-pyrazol-4-yl)phenyl)-1,2,3,4-tetrahydroisoquinoline-3-carboxamide (35). 1H NMR (CH_3CN-d_3 , 400 MHz) δ 1.83–2.11 (m, 4H), 2.74 (s, 3H), 2.82–2.92 (m, 1H), 3.20–3.32 (m, 1H), 3.39 (dd, J = 16.6, 4.5 Hz, 1H), 3.44–3.53 (m, 2H), 3.78 (s, 3H), 3.95–4.03 (m, 1H), 4.38 (q, J = 15.4 Hz, 2H), 4.50–4.62 (m, 1H), 6.80 (d, J = 2.0 Hz, 1H), 6.87 (dd, J = 2.4, 8.5 Hz, 1H), 7.05–7.21 (m, 3H), 7.83 (d, J = 8.0 Hz, 1H), 7.92 (bs, 2H), 8.95 (s, 1H), 10.61 (bs, 1H). ^{13}C NMR (CH_3CN-d_3 , 100 MHz) δ 26.7, 26.9, 31.0, 33.9, 44.0, 44.6, 55.1, 56.0, 56.2, 72.7, 110.2, 114.3, 114.4, 121.3, 124.1, 125.1, 128.7, 133.6, 146.8, 150.9, 160.3. Single peak in analytical HPLC. LC-MS (ESI): m/z 476 $[M + 1]^+$. HRMS (ESI-Orbitrap), MH^+ calcd for $C_{27}H_{33}N_5O_3$, 476.2683; found, 476.2655.

(*R*)-*N*-(4-(1*H*-Pyrazol-4-yl)-2-(2-(pyrrolidin-1-yl)ethoxy)phenyl)-6-methoxy-1,2,3,4-tetrahydro-isoquinoline-3-carboxamide (36). ¹H NMR (CH₃CN-*d*₃, 400 MHz) δ 2.00–2.11 (m, 4H), 2.74 (s, 2H), 3.24–3.34 (m, 1H), 3.43 (dd, *J* = 16.8, 4.8 Hz, 1H), 3.55–3.66 (m, 2H), 3.78 (s, 3H), 4.31–4.45 (m, 4H), 4.56 (dd, *J* = 11.1, 4.9 Hz, 1H), 6.78–6.80 (m, 1H), 6.87 (dd, *J* = 2.5, 8.6 Hz, 1H), 7.13–7.21 (m, 3H), 7.85–7.93 (m, 2H), 9.72 (s, 1H). ¹³C NMR (CH₃CN-*d*₃, 100 MHz) δ 23.8, 30.8, 38.8, 44.7, 54.8, 56.0, 56.4, 64.7, 110.8, 114.2, 114.4, 119.4, 121.2, 124.4, 125.5, 128.7, 131.8, 133.7, 149.9, 160.2, 168.0. Single peak in analytical HPLC. LC-MS (ESI): *m/z* 462 [M + 1]⁺. HRMS (ESI-Orbitrap), MH⁺ calcd for C₂₆H₃₁N₅O₃, 462.2527; found, 462.2498.

(*R*)-6-Methoxy-*N*-(2-(1-methylpiperidin-4-yloxy)-4-(1*H*-pyrazol-4-yl)phenyl)-1,2,3,4-tetrahydro-isoquinoline-3-carboxamide (37). ¹H NMR (DMSO-*d*₆, 400 MHz) δ 2.75–2.64 (m, 1H), 2.92–2.86 (m, 1H), 2.96 (s, 6H), 3.17–3.04 (m, 1H), 3.33 (dd, *J* = 17.0, 4.3 Hz, 1H), 3.58 (s, 1H), 3.76 (s, 3H), 3.87–3.78 (m, 1H), 4.54–4.25 (m, 4H), 7.01–6.86 (m, 3H), 7.40–7.13 (m, 4H), 7.80–7.73 (m, 1H), 8.11–8.03 (m, 2H). ¹³C NMR (CH₃CN-*d*₃, 100 MHz) δ 27.9, 30.9, 42.6, 44.9, 50.4, 52.5, 56.0, 56.4, 67.9, 71.4, 110.9, 112.5, 114.3, 114.5, 119.5, 120.8, 124.7, 125.3, 125.6, 126.3, 128.8, 133.2, 149.4, 160.4, 167.7. Single peak in analytical HPLC. LC-MS (ESI): *m/z* 462 [M + 1]⁺. HRMS (ESI-Orbitrap), MH⁺ calcd for C₂₆H₃₁N₅O₃, 462.2527; found, 462.2499.

(*R*)-6-Methoxy-*N*-(2-(2-methoxyethoxy)-4-(1*H*-pyrazol-4-yl)-phenyl)-1,2,3,4-tetrahydroisoquinoline-3-carboxamide (38). ¹H NMR (MeOH-*d*₄, 400 MHz) δ 2.72–2.64 (m, 1H), 3.03 (s, 6H), 3.18–3.10 (m, 1H), 3.57 (dd, *J* = 17.0, 4.6 Hz, 1H), 3.83–3.66 (m, 2H), 4.48 (dd, *J* = 30.5, 15.5 Hz, 2H), 4.64–4.57 (m, 2H), 4.68 (dd, *J* = 12.1, 5.1 Hz, 2H), 7.13–7.05 (m, 2H), 7.32 (dd, *J* = 9.1, 5.0 Hz, 1H), 7.60 (d, *J* = 6.8 Hz, 1H), 8.02–7.99 (m, 2H), 8.30 (d, *J* = 6.8 Hz, 1H), 8.45 (d, *J* = 9.0 Hz, 1H). Single peak in analytical HPLC. LC-MS (ESI): *m/z* 423 [M + 1]⁺. HRMS (ESI-Orbitrap), MH⁺ calcd for C₂₃H₂₆N₄O₄, 423.2053; found, 423.2025.

(*R*)-*N*-(2-(2-Hydroxyethoxy)-4-(1*H*-pyrazol-4-yl)phenyl)-6-methoxy-1,2,3,4-tetrahydroisoquinoline-3-carboxamide (39). ¹H NMR (MeOH-*d*₄, 400 MHz) δ 2.72–2.64 (m, 1H), 3.03 (s, 6H), 3.18–3.10 (m, 1H), 3.57 (dd, *J* = 17.0, 4.6 Hz, 1H), 3.83–3.66 (m, 2H), 4.48 (dd, *J* = 30.5, 15.5 Hz, 2H), 4.64–4.57 (m, 2H), 4.68 (dd, *J* = 12.1, 5.1 Hz, 2H), 7.13–7.05 (m, 2H), 7.32 (dd, *J* = 9.1, 5.0 Hz, 1H), 7.60 (d, *J* = 6.8 Hz, 1H), 8.02–7.99 (m, 2H), 8.30 (d, *J* = 6.8 Hz, 1H), 8.45 (d, *J* = 9.0 Hz, 1H). Single peak in analytical HPLC. LC-MS (ESI): *m/z* 409 [M + 1]⁺.

(*R*)-*N*-(2-(2-(Dimethylamino)ethylthio)-4-(1*H*-pyrazol-4-yl)-phenyl)-6-methoxy-1,2,3,4-tetrahydroisoquinoline-3-carboxamide (40). ¹H NMR (MeOH-*d*₄, 400 MHz) δ 2.93 (s, 6H), 3.07–3.18 (m, 1H), 3.37–3.45 (m, 1H), 3.59 (dd, *J* = 16.9, 4.7 Hz, 1H), 3.84 (s, 3H), 4.47 (s, 2H), 4.50–4.57 (m, 1H), 6.91–6.98 (m, 1H), 7.24 (d, *J* = 8.2 Hz, 1H), 7.59–7.69 (m, 2H), 7.87–7.91 (m, 1H), 8.09 (s, 2H). Single peak in analytical HPLC. LC-MS (ESI): *m/z* 452 [M + 1]⁺. HRMS (ESI-Orbitrap), MH⁺ calcd for C₂₄H₂₉N₅O₂S, 452.2142; found, 452.2111.

(*R*)-*N*-(2-(2-(Dimethylamino)ethylthio)-4-(3-methyl-1*H*-pyrazol-4-yl)phenyl)-6-methoxy-1,2,3,4-tetrahydroisoquinoline-3-carboxamide (41). ¹H NMR (MeOH-*d*₄, 400 MHz) δ 2.35 (s, 3H), 2.79–2.81 (m, 6H), 3.05–3.01 (m, 1H), 3.40–3.26 (m, 1H), 3.46 (dd, *J* = 16.7, 4.6 Hz, 1H), 3.72 (s, 3H), 4.31–4.44 (m, 3H), 6.79–6.86 (m, 2H), 7.12 (d, *J* = 8.3 Hz, 1H), 7.40 (dd, *J* = 8.4, 2.0 Hz, 1H), 7.53 (d, *J* = 8.3 Hz, 1H), 7.61 (d, *J* = 1.7 Hz, 1H), 7.70 (s, 1H). LC-MS (ESI): *m/z* 466 [M + 1]⁺. HRMS (ESI-Orbitrap), MH⁺ calcd for C₂₅H₃₁N₅O₂S, 466.2298; found, 466.2269.

(*R*)-*N*-(2-(4-(Dimethylamino)-4-oxobutylthio)-4-(3-methyl-1*H*-pyrazol-4-yl)phenyl)-6-methoxy-1,2,3,4-tetrahydroisoquinoline-3-carboxamide (42). ¹H NMR (MeOH-*d*₄, 400 MHz) δ 2.65–2.58 (m, 2H), 2.73 (s, 3H), 2.95 (s, 3H), 3.10–3.03 (m, 2H), 3.34–3.26 (m, 1H), 3.54 (dd, *J* = 16.66, 5.07 Hz, 1H), 3.78 (s, 3H), 4.45–4.37 (m, 2H), 4.75 (dd, *J* = 10.44, 5.04 Hz, 1H), 6.90–6.83 (m, 2H), 7.18 (d, *J* = 8.48 Hz, 1H), 7.59 (dd, *J* = 8.49, 2.12 Hz, 1H), 7.85 (d,

J = 2.11 Hz, 1H), 7.93 (s, 2H), 8.18 (d, *J* = 8.53 Hz, 1H), 10.47 (s, 1H). LC-MS (ESI): *m/z* 480 [M + 1]⁺. HRMS (ESI-Orbitrap), MH⁺ calcd for C₂₅H₂₉N₅O₃S, 480.2090; found, 480.2063.

(*R*)-*N*-(2-(2-(Dimethylamino)ethoxy)-3-fluoro-4-(1*H*-pyrazol-4-yl)phenyl)-6-methoxy-1,2,3,4-tetrahydroisoquinoline-3-carboxamide (43). ¹H NMR (DMSO-*d*₆, 400 MHz) δ 2.55–2.64 (m, 1H), 2.82–2.89 (m, 1H), 2.94 (s, 6H), 3.17–3.04 (m, 1H), 3.33 (dd, *J* = 17.0, 4.3 Hz, 1H), 3.58 (s, 1H), 3.69 (s, 3H), 3.67–3.78 (m, 1H), 4.24–4.55 (m, 4H), 6.86 (m, 3H), 7.10–7.19 (m, 4H), 7.70–7.73 (m, 1H), 8.11 (s, 2H). Single peak in analytical HPLC. LC-MS (ESI): *m/z* 454 [M + 1]⁺. HRMS (ESI-Orbitrap), MH⁺ calcd for C₂₄H₂₈FN₅O₃, 454.2276; found, 454.2246.

(*R*)-*N*-(2-(2-(Dimethylamino)ethoxy)-5-fluoro-4-(1*H*-pyrazol-4-yl)phenyl)-6-methoxy-1,2,3,4-tetrahydroisoquinoline-3-carboxamide (44). ¹H NMR (DMSO-*d*₆, 400 MHz) δ 2.95 (s, 6H), 3.13 (dd, *J* = 16.3, 12.4 Hz, 1H), 3.39 (dd, *J* = 16.8, 4.4 Hz, 1H), 3.66–3.60 (m, 2H), 3.76 (s, 3H), 4.33 (q, *J* = 15.6 Hz, 2H), 4.51 (t, *J* = 5.0 Hz, 3H), 6.93–6.83 (m, 2H), 7.22 (d, *J* = 8.6 Hz, 1H), 7.49 (d, *J* = 7.0 Hz, 1H), 7.88 (dd, *J* = 12.5, 4.6 Hz, 1H), 8.11 (d, *J* = 1.6 Hz, 2H), 9.68 (s, 1H), 10.05–9.86 (m, 2H), 10.24 (s, 1H). Single peak in analytical HPLC. LC-MS (ESI): *m/z* 454 [M + 1]⁺. HRMS (ESI-Orbitrap), MH⁺ calcd for C₂₄H₂₈FN₅O₃, 454.2276; found, 454.2246.

(*R*)-*N*-(2-(2-(Dimethylamino)ethoxy)-6-fluoro-4-(1*H*-pyrazol-4-yl)phenyl)-6-methoxy-1,2,3,4-tetrahydroisoquinoline-3-carboxamide (45). ¹H NMR (DMSO-*d*₆, 400 MHz) δ 2.96 (s, 6H), 3.17–3.04 (m, 2H), 3.28–3.33 (m, 2H), 3.58 (s, 1H), 3.77 (s, 3H), 3.87–3.78 (m, 1H), 4.54–4.25 (m, 3H), 6.86–6.98 (m, 3H), 7.40–7.53 (m, 4H), 7.70–7.73 (m, 1H), 8.14 (s, 2H). Single peak in analytical HPLC. LC-MS (ESI): *m/z* 454 [M + 1]⁺. HRMS (ESI-Orbitrap), MH⁺ calcd for C₂₄H₂₈FN₅O₃, 454.2276; found, 454.2246.

(*R*)-*N*-(2-(2-(Dimethylamino)ethoxy)-5-fluoro-4-(1*H*-pyrazol-4-yl)phenyl)-1,2,3,4-tetrahydroisoquinoline-3-carboxamide (46). ¹H NMR (DMSO-*d*₆, 400 MHz) δ 2.93 (s, 6H), 3.14 (dd, *J* = 12.4, 16.8 Hz, 1H), 3.45 (dd, *J* = 4.4, 16.8 Hz, 1H), 3.60 (s, 2H), 4.41 (m, 2H), 4.49 (m, 3H), 7.28 (m, 4H), 7.48 (d, *J* = 6.8 Hz, 1H), 7.87 (d, *J* = 12.4 Hz, 1H), 8.10 (s, 2H), 9.62 (b, 1H), 9.80 (b, 1H), 10.00 (s, 1H), 10.10 (b, 1H). Single peak in analytical HPLC. LC-MS (ESI): *m/z* 424 [M + 1]⁺. HRMS (ESI-Orbitrap), MH⁺ calcd for C₂₃H₂₆FN₅O₂, 424.2170; found, 424.2141.

General Procedure C: (*R*)-*N*-(2-(2-(Dimethylamino)ethoxy)-5-fluoro-4-(1*H*-pyrazol-4-yl)phenyl)-2-methyl-1,2,3,4-tetrahydroisoquinoline-3-carboxamide (47). (*R*)-*N*-(4-bromo-2-(2-(dimethylamino)ethoxy)-5-fluorophenyl)-1,2,3,4-tetrahydroisoquinoline-3-carboxamide was synthesized according to the first step in general procedure A. The Boc group was removed by treatment with 1:1 TFA/CH₂Cl₂ (10 mL) in the presence of 5% of TIS. After concentration, the residue was dissolved in EtOAc, washed with saturated NaHCO₃ and brine, and dried over anhydrous Na₂SO₄. Filtration and removal of solvent under reduced pressure provided the crude bromo-amide.

To the solution of the intermediate from last step (87 mg, 0.2 mmol) in CH₂Cl₂, formaldehyde (6 mg, 0.2 mmol) was added and the reaction mixture was stirred for 5 min. Then, sodium triacetoxyborohydride (64 mg, 0.3 mmol) was added, and the reaction was stirred overnight. Extra NaBH₄ (7 mg, 0.2 mmol) was added to complete the reduction of imine. The reaction was quenched by addition of methanol. After concentration, the residue was dissolved in EtOAc, washed with 1 M NaOH solution, brine, saturated NaHCO₃ solution, and brine, and dried over anhydrous Na₂SO₄. It was filtered and concentrated to provide the crude product amide, which was used in the next step without purification.

Thus, pyrazole boronic pinacol ester (54 mg, 0.28 mmol), K₂CO₃ (111 mg, 0.8 mmol), and palladium tetrakis(triphenylphosphine) (23 mg, 0.02 mmol) were added consequently to a solution of the amide from the last step in 4:1 dioxane/water (2 mL). The reaction mixture was sealed in a microwave vial, degassed under vacuum, and charged with argon. It was then heated in a

microwave oven at 140 °C for 30 min. All solvent was removed and the residue was diluted with EtOAc, which was washed with NaHCO₃ solution and brine. After concentration, the residue was subjected to preparative HPLC to provide **47** as a fine powder of its TFA salt. ¹H NMR (DMSO-*d*₆, 400 MHz) δ 2.39 (s, 1H), 2.93 (s, 6H), 3.12 (dd, *J* = 11.4, 16.8 Hz, 1H), 3.45 (dd, *J* = 4.4, 16.8 Hz, 1H), 3.60 (s, 2H), 4.40–4.42 (m, 2H), 4.45–4.48 (m, 3H), 7.26–7.28 (m, 4H), 7.58 (d, *J* = 5.8 Hz, 1H), 7.81 (d, *J* = 12.4 Hz, 1H), 8.01 (s, 2H), 9.60 (b, 1H), 9.81 (b, 1H), 10.00–10.10 (m, 2H). Single peak in analytical HPLC. LC-MS (ESI): *m/z* 438 [M + 1]⁺. HRMS (ESI-Orbitrap), MH⁺ calcd for C₂₄H₂₈FN₅O₂, 438.2326; found, 438.2297.

Compounds **47–50** were prepared according to General Procedure C:

(R)-N-(2-(2-(Dimethylamino)ethoxy)-5-fluoro-4-(1H-pyrazol-4-yl)phenyl)-2-ethyl-1,2,3,4-tetrahydroisoquinoline-3-carboxamide (48). ¹H NMR (DMSO-*d*₆, 400 MHz) δ 1.18 (t, 3H), 2.39 (m, 2H), 2.87 (s, 6H), 3.10–3.14 (m, 1H), 3.45 (dd, *J* = 4.0, 14.8 Hz, 1H), 3.61 (s, 2H), 4.41–4.43 (m, 2H), 4.39–4.42 (m, 3H), 7.20–7.24 (m, 4H), 7.48 (d, *J* = 5.8 Hz, 1H), 7.87 (d, *J* = 12.1 Hz, 1H), 8.12 (s, 2H), 9.52 (b, 1H), 9.90–9.92 (m, 2H), 10.10 (b, 1H). Single peak in analytical HPLC. LC-MS (ESI): *m/z* 452 [M + 1]⁺. HRMS (ESI-Orbitrap), MH⁺ calcd for C₂₅H₃₀FN₅O₂, 452.2483; found, 452.2454.

(R)-2-(Cyclopropylmethyl)-N-(2-(2-(dimethylamino)ethoxy)-5-fluoro-4-(1H-pyrazol-4-yl)phenyl)-1,2,3,4-tetrahydroisoquinoline-3-carboxamide (49). ¹H NMR (MeOH-*d*₄, 400 MHz) δ 0.49–0.53 (m, 5H), 2.41 (m, 1H), 2.98 (s, 6H), 3.14 (m, 1H), 3.45 (m, 1H), 3.60 (s, 2H), 4.41–4.43 (m, 2H), 4.48–4.50 (m, 3H), 7.25–7.28 (m, 4H), 7.48 (d, *J* = 6.8 Hz, 1H), 7.87 (m, 1H), 8.10 (s, 2H), 10.00 (s, 1H). Single peak in analytical HPLC. LC-MS (ESI): *m/z* 478 [M + 1]⁺. HRMS (ESI-Orbitrap), MH⁺ calcd for C₂₇H₃₂FN₅O₂, 478.2639; found, 478.2613.

(R)-N-(2-(2-(Dimethylamino)ethoxy)-4-(1H-pyrazol-4-yl)phenyl)-2-ethyl-1,2,3,4-tetrahydroisoquinoline-3-carboxamide (51). ¹H NMR (DMSO-*d*₆, 400 MHz) δ 1.10 (t, 3H), 2.40 (m, 1H), 2.98 (s, 6H), 3.04 (dd, *J* = 11.4, 15.9 Hz, 1H), 3.35 (dd, *J* = 4.4, 15.9 Hz, 1H), 3.60 (s, 2H), 4.38–4.40 (m, 2H), 4.52–4.54 (m, 3H), 7.21–7.25 (m, 4H), 7.48 (d, *J* = 6.5 Hz, 1H), 7.87 (d, *J* = 12.0 Hz, 1H), 8.10 (s, 2H), 9.62 (b, 1H), 9.80 (b, 1H), 9.90–10.00 (m, 2H). Single peak in analytical HPLC. LC-MS (ESI): *m/z* 464 [M + 1]⁺. HRMS (ESI-Orbitrap), MH⁺ calcd for C₂₆H₃₃N₅O₃, 464.2683; found, 464.2655.

ROCK-I/II Assays. Assays were performed using the STK2 kinase system from Cisbio. A 5 μL mixture of a 1 μM STK2 substrate and ATP (ROCK-I: 4 μM, ROCK-II: 20 μM) in STK-buffer was added to the wells using a BioRAPTR FRD Workstation (Aurora Discovery). Then 20 nL of test compounds was dispensed. Reaction was started by the addition of 5 μL of 2.5 nM ROCK-I (Upstate no. 14-601) or 0.5 nM ROCK-II in STK-buffer. After 4 h at rt, the reaction was stopped by addition of 10 μL of 1× antibody and 62.5 nM Sa-XL in detection buffer. After 1 h at rt, the plates were read on the Viewlux in HTRF mode.

PKA Assays. First, 5 μL mixture of a 60 μM kemptide and 20 μM ATP in kinase buffer (50 mM Hepes pH 7.3, 10 mM MgCl₂, 0.1% BSA, 2 mM DTT) were added to the wells using a BioRAPTR FRD Workstation (Aurora Discovery). Then 20 nL of test compounds was dispensed. Reaction was started by addition of 5 μL of 0.5 nM PKA (Upstate no. 14-440) in kinase buffer (5 μL of kinase buffer for high wells). After 70 min at rt, the reaction was stopped by addition of 10 μL of Kinase-Glo reagent and the plate was read after 10 min incubation time at rt on the Viewlux in luminescence mode.

ppMLC Cell-Based Assays. Detection of Bisphospho-MLC2-Modulation by In-cell Western using the LI-COR Odyssey Infrared Imaging System. Bisphospho-MLC2 levels in A7r5 cells (purchased from ATCC, Manassas, VA) was detected and quantified as previously described.³⁰ Briefly, A7r5 cells were plated at 5000 cells/well in a 96-well Packard view plate (Perkin-Elmer) in DMEM + 10%

FBS. Following attachment, cells were serum starved for 4 h and treated with inhibitor in 0.25% DMSO (final concentration) for 1 h at 37 °C. Cells were then treated with 10 μM LPA for 10 min, fixed with 4% paraformaldehyde for 30 min, washed in PBS + 0.1 M glycine, and permeabilized in 0.2% Triton X for 10 min. Cells were then washed once in PBS and blocked in LI-COR blocking buffer (LI-COR Biosciences) for 1 h at 25 °C. Cells were probed for phosphorylated myosin light chain 20 using 55 ng/mL of primary rabbit antibody and incubated overnight at 4 °C. Following three washes, cells were probed with goat-antirabbit IR800 antibody (2 μg/mL in LI-COR blocking buffer + 0.025% Tween-20) for 1 h at 25 °C. Nuclei were stained with TO-PRO-3 iodide (642/661) (Invitrogen, Carlsbad, CA) (1:4000) for 20 min, washed twice in PBS/0.05% Tween-20, and read with an Odyssey infrared imaging system (LI-COR Biosciences).

Determination of IOP in a Rat Model. An elevated rat IOP model was used to evaluate the IOP lowering effects of compounds. We have previously utilized this method for evaluating IOP lowering in rats to assess other ROCK inhibitors.²⁶ Initial IOP was 29 mmHg. The IOP was measured in Brown Norway rats that were housed in constant low-light conditions to reduce circadian IOP changes. Measurements were made using a rebound tonometer with *n* = 7 in the vehicle and drug treated groups. The reported ΔIOP (IOP decrease relative to vehicle) at each time point is the average of five readings. Compounds were formulated in 50 mM citrate buffer, pH = 5.5 w/v.

Acknowledgment. We thank Professors Patrick Griffin and William R. Roush for their support. We are grateful to Dr. Derek Duckett and Weimin Chen for p38 and JNK assays, and to Dr. Michael Chalmers for HRMS. We acknowledge the resources from the University of Miami Center for Computational Science.

Supporting Information Available: Compound purity data by analytical HPLC for key compounds, chirality assignments by ¹H NMR of Mosher amides for those pairs of *R* and *S* enantiomers, and the kinase panel screening data for compound **35**. This material is available free of charge via the Internet at <http://pubs.acs.org>.

References

- (1) Nakagawa, O.; Fujisawa, K.; Ishizaki, T.; Saito, Y.; Nakao, K.; Narumiya, S. ROCK-I and ROCK-II, two isoforms of Rho-associated coiled-coil forming protein serine/threonine kinase in mice. *FEBS Lett.* **1996**, *392* (2), 189–193.
- (2) Ishizaki, T.; Naito, M.; Fujisawa, K.; Maekawa, M.; Watanabe, N.; Saito, Y.; Narumiya, S. p160(ROCK), a Rho-associated coiled-coil forming protein kinase, works downstream of Rho and induces focal adhesions. *FEBS Lett.* **1997**, *404* (2–3), 118–124.
- (3) Uehata, M.; Ishizaki, T.; Satoh, H.; Ono, T.; Kawahara, T.; Morishita, T.; Tamakawa, H.; Yamagami, K.; Inui, J.; Maekawa, M.; Narumiya, S. Calcium sensitization of smooth muscle mediated by a Rho-associated protein kinase in hypertension. *Nature* **1997**, *389* (6654), 990–994.
- (4) Kubo, T.; Hata, K.; Yamaguchi, A.; Yamashita, T. Rho-ROCK inhibitors as emerging strategies to promote nerve regeneration. *Curr. Pharm. Des.* **2007**, *13* (24), 2493–2499.
- (5) Satoh, S.; Tushima, Y.; Ikegaki, I.; Iwasaki, M.; Asano, T. Wide therapeutic time window for fasudil neuroprotection against ischemia-induced delayed neuronal death in gerbils. *Brain Res.* **2007**, *1128* (1), 175–180.
- (6) Doe, C.; Bentley, R.; Behm, D. J.; Lafferty, R.; Stavenger, R.; Jung, D.; Bamford, M.; Panchal, T.; Grygielko, E.; Wright, L. L.; Smith, G. K.; Chen, Z. X.; Webb, C.; Khandekar, S.; Yi, T.; Kirkpatrick, R.; Dul, E.; Jolivet, L.; Marino, J. P.; Willette, R.; Lee, D.; Hu, E. D. Novel Rho kinase inhibitors with anti-inflammatory and vasodilatory activities. *J. Pharmacol. Exp. Ther.* **2007**, *320* (1), 89–98.
- (7) Hirooka, Y.; Shimokawa, H.; Takeshita, A. Rho-kinase, a potential therapeutic target for the treatment of hypertension. *Drug News Perspect.* **2004**, *17* (8), 523–527.
- (8) Bivalacqua, T. J.; Champion, H. C.; Usta, M. F.; Celtek, S.; Chitale, K.; Webb, R. C.; Lewis, R. L.; Mills, T. M.; Hellstrom,

- W. J. G.; Kadowitz, P. J. RhoA/Rho-kinase suppresses endothelial nitric oxide synthase in the penis: a mechanism for diabetes-associated erectile dysfunction. *Proc. Natl. Acad. Sci. U.S.A.* **2004**, *101* (24), 9121–9126.
- (9) Waki, M.; Yoshida, Y.; Oka, T.; Azuma, M. Reduction of intraocular pressure by topical administration of an inhibitor of the Rho-associated protein kinase. *Curr. Eye Res.* **2001**, *22* (6), 470–474.
- (10) Nakajima, M.; Hayashi, K.; Egi, Y.; Katayama, K.; Amano, Y.; Uehata, M.; Ohtsuki, M.; Fujii, A.; Oshita, K.; Kataoka, H.; Chiba, K.; Goto, N.; Kondo, T. Effect of Wf-536, a novel ROCK inhibitor, against metastasis of B16 melanoma. *Cancer Chemother. Pharmacol.* **2003**, *52* (4), 319–324.
- (11) Nakajima, M.; Hayashi, K.; Katayama, K.; Amano, Y.; Egi, Y.; Uehata, M.; Goto, N.; Kondo, T. Wf-536 prevents tumor metastasis by inhibiting both tumor motility and angiogenic actions. *Eur. J. Pharmacol.* **2003**, *459* (2–3), 113–120.
- (12) Chan, C. C. M.; Khodarahmi, K.; Liu, J.; Sutherland, D.; Oschipok, L. W.; Steeves, J. D.; Tetzlaff, W. Dose-dependent beneficial and detrimental effects of ROCK inhibitor Y27632 on axonal sprouting and functional recovery after rat spinal cord injury. *Exp. Neurol.* **2005**, *196* (2), 352–364.
- (13) Sun, X. J.; Minohara, M.; Kikuchi, H.; Ishizu, T.; Tanaka, M.; Piao, H.; Osoegawa, M.; Ohyagi, Y.; Shimokawa, H.; Kira, J. The selective Rho-kinase inhibitor Fasudil is protective and therapeutic in experimental autoimmune encephalomyelitis. *J. Neuroimmunol.* **2006**, *180* (1–2), 126–134.
- (14) LoGrasso, P. V.; Feng, Y. B. Rho Kinase (ROCK) Inhibitors and Their Application to Inflammatory Disorders. *Curr. Top. Med. Chem.* **2009**, *9* (8), 704–723.
- (15) Asano, T.; Ikegaki, I.; Satoh, S. I.; Suzuki, Y.; Shibuya, M.; Takayasu, M.; Hidaka, H. Mechanism of action of a novel antivasospasm drug, ha1077. *J. Pharmacol. Exp. Ther.* **1987**, *241* (3), 1033–1040.
- (16) Iwakubo, M.; Takami, A.; Okada, Y.; Kawata, T.; Tagami, Y.; Sato, M.; Sugiyama, T.; Fukushima, K.; Taya, S.; Amano, M.; Kaibuchi, K.; Iijima, H. Design and synthesis of rho kinase inhibitors (III). *Bioorg. Med. Chem.* **2007**, *15* (2), 1022–1033.
- (17) Takami, A.; Iwakubo, M.; Okada, Y.; Kawata, T.; Odai, H.; Takahashi, N.; Shindo, K.; Kimura, K.; Tagami, Y.; Miyake, M.; Fukushima, K.; Inagaki, M.; Amano, M.; Kaibuchi, K.; Iijima, H. Design and synthesis of Rho kinase inhibitors (I). *Bioorg. Med. Chem.* **2004**, *12* (9), 2115–2137.
- (18) Stavenger, R. A.; Cui, H. F.; Dowdell, S. E.; Franz, R. G.; Gaitanopoulos, D. E.; Goodman, K. B.; Hilfiker, M. A.; Ivy, R. L.; Leber, J. D.; Marino, J. P.; Oh, H. J.; Viet, A. Q.; Xu, W. W.; Ye, G. S.; Zhang, D. H.; Zhao, Y. D.; Jolivet, L. J.; Head, M. S.; Semus, S. F.; Elkins, P. A.; Kirkpatrick, R. B.; Dul, E.; Khandekar, S. S.; Yi, T.; Jung, D. K.; Wright, L. L.; Smith, G. K.; Behm, D. J.; Doe, C. P.; Bentley, R.; Chen, Z. X.; Hu, E. D.; Lee, D. Discovery of aminofurazan-azabenzimidazoles as inhibitors of Rho-kinase with high kinase selectivity and antihypertensive activity. *J. Med. Chem.* **2007**, *50* (1), 2–5.
- (19) Sehon, C. A.; Wang, G. Z.; Viet, A. Q.; Goodman, K. B.; Dowdell, S. E.; Elkins, P. A.; Semus, S. F.; Evans, C.; Jolivet, L. J.; Kirkpatrick, R. B.; Dul, E.; Khandekar, S. S.; Yi, T.; Wright, L. L.; Smith, G. K.; Behm, D. J.; Bentley, R.; Doe, C. P.; Hu, E.; Lee, D. Potent, selective and orally bioavailable dihydropyrimidine inhibitors of Rho kinase (ROCK1) as potential therapeutic agents for cardiovascular diseases. *J. Med. Chem.* **2008**, *51* (21), 6631–6634.
- (20) Feng, Y. B.; Cameron, M. D.; Frackowiak, B.; Griffin, E.; Lin, L.; Ruiz, C.; Schroter, T.; LoGrasso, P. Structure–activity relationships, and drug metabolism and pharmacokinetic properties for indazole piperazine and indazole piperidine inhibitors of ROCK-II. *Bioorg. Med. Chem. Lett.* **2007**, *17* (8), 2355–2360.
- (21) Schirok, H.; Kast, R.; Figueroa-Perez, S.; Bennabi, S.; Gnoth, M. J.; Feurer, A.; Heckroth, H.; Thutewohl, M.; Paulsen, H.; Knorr, A.; Huetter, J.; Lobell, M.; Muentner, K.; Geiss, V.; Ehmke, H.; Lang, D.; Radtke, M.; Mittendorf, J.; Stasch, J. P. Design and Synthesis of Potent and Selective Azaindole-Based Rho Kinase (ROCK) Inhibitors. *ChemMedChem* **2008**, *3* (12), 1893–1904.
- (22) Feng, Y. B.; Yin, Y.; Weiser, A.; Griffin, E.; Cameron, M. D.; Lin, L.; Ruiz, C.; Schurer, S. C.; Inoue, T.; Rao, P. V.; Schroter, T.; LoGrasso, P. Discovery of Substituted 4-(Pyrazol-4-yl)-phenylbenzodioxane-2-carboxamides as Potent and Highly Selective Rho Kinase (ROCK-II) Inhibitors. *J. Med. Chem.* **2008**, *51* (21), 6642–6645.
- (23) Chen, Y. T.; Bannister, T. D.; Weiser, A.; Griffin, E.; Lin, L.; Ruiz, C.; Cameron, M. D.; Schurer, S.; Duckett, D.; Schroter, T.; LoGrasso, P.; Feng, Y. B. Chroman-3-amides as potent Rho kinase inhibitors. *Bioorg. Med. Chem. Lett.* **2008**, *18* (24), 6406–6409.
- (24) Sessions, E. H.; Yin, Y.; Bannister, T. D.; Weiser, A.; Griffin, E.; Pocas, J.; Cameron, M. D.; Ruiz, C.; Lin, L.; Schurer, S. C.; Schroter, T.; LoGrasso, P.; Feng, Y. B. Benzimidazole- and benzoxazole-based inhibitors of Rho kinase. *Bioorg. Med. Chem. Lett.* **2008**, *18* (24), 6390–6393.
- (25) Yin, Y.; Lin, L.; Ruiz, C.; Cameron, M. D.; Pocas, J.; Grant, W.; Schroter, T.; Chen, W. M.; Duckett, D.; Schurer, S.; LoGrasso, P.; Feng, Y. B. Benzothiazoles as Rho-associated kinase (ROCK-II) inhibitors. *Bioorg. Med. Chem. Lett.* **2009**, *19* (23), 6686–6690.
- (26) Yin, Y.; Cameron, M. D.; Lin, L.; Khan, S.; Schroter, T.; Grant, W.; Pocas, J.; Chen, Y. T.; Schurer, S.; Pachori, A.; LoGrasso, P.; Feng, Y. Discovery of Potent and Selective Urea-Based ROCK Inhibitors and Their Effects on Intraocular Pressure in Rats. *ACS Med. Chem. Lett.* **2010**, *1*, 175–179.
- (27) AbdelMagid, A. F.; Carson, K. G.; Harris, B. D.; Maryanoff, C. A.; Shah, R. D. Reductive amination of aldehydes and ketones with sodium triacetoxyborohydride. Studies on direct and indirect reductive amination procedures. *J. Org. Chem.* **1996**, *61* (11), 3849–3862.
- (28) Ortwine, D. F.; Malone, T. C.; Bigge, C. F.; Drummond, J. T.; Humblet, C.; Johnson, G.; Pinter, G. W. Generation of *N*-Methyl-D-aspartate Agonist and Competitive Antagonist Pharmacophore Models—Design and Synthesis of Phosphonoalkyl-Substituted Tetrahydroisoquinolines as Novel Antagonists. *J. Med. Chem.* **1992**, *35* (8), 1345–1370.
- (29) Schroeter, T.; Minond, D.; Weiser, A.; Dao, C.; Habel, J.; Spicer, T.; Chase, P.; Baillargeon, P.; Scampavia, L.; Schuerer, S.; Chung, C.; Mader, C.; Southern, M.; Tsinoemas, N.; LoGrasso, P.; Hodder, P. Comparison of miniaturized time-resolved fluorescence resonance energy transfer and enzyme-coupled luciferase high-throughput screening assays to discover inhibitors of Rho-kinase II (ROCK-II). *J. Biomol. Screen.* **2008**, *13* (1), 17–28.
- (30) Schroter, T.; Griffin, E.; Weiser, A.; Feng, Y. B.; LoGrasso, P. Detection of myosin light chain phosphorylation—a cell-based assay for screening Rho-kinase inhibitors. *Biochem. Biophys. Res. Commun.* **2008**, *374* (2), 356–360.
- (31) Breitenlechner, C.; Gassel, M.; Hidaka, H.; Kinzel, V.; Huber, R.; Engh, R. A.; Bossemeyer, D. Protein kinase a in complex with rho-kinase inhibitors Y-27632, fasudil, and H-1152P: structural basis of selectivity. *Structure* **2003**, *11* (12), 1595–1607.
- (32) Tamura, M.; Nakao, H.; Yoshizaki, H.; Shiratsuchi, M.; Shigyo, H.; Yamada, H.; Ozawa, T.; Totsuka, J.; Hidaka, H. Development of specific Rho-kinase inhibitors and their clinical application. *Biochim. Biophys. Acta, Proteins Proteomics* **2005**, *1754* (1–2), 245–252.
- (33) Hoye, T. R.; Renner, M. K. MTPA (Mosher) amides of cyclic secondary amines: conformational aspects and a useful method for assignment of amine configuration. *J. Org. Chem.* **1996**, *61* (6), 2056–2064.
- (34) Zhou, P.; Zou, J. W.; Tian, F. F.; Shang, Z. C. Fluorine Bonding—How Does It Work In Protein–Ligand Interactions? *J. Chem. Inf. Model.* **2009**, *49* (10), 2344–2355.
- (35) Christopher, J. A.; Atkinson, F. L.; Bax, B. D.; Brown, M. J. B.; Champigny, A. C.; Chuang, T. T.; Jones, E. J.; Mosley, J. E.; Musgrave, J. R. 1-Aryl-3,4-dihydroisoquinoline inhibitors of JNK3. *Bioorg. Med. Chem. Lett.* **2009**, *19* (8), 2230–2234.
- (36) Hagmann, W. K. The many roles for fluorine in medicinal chemistry. *J. Med. Chem.* **2008**, *51* (15), 4359–4369.
- (37) Bohm, H. J.; Banner, D.; Bendels, S.; Kansy, M.; Kuhn, B.; Muller, K.; Obst-Sander, U.; Stahl, M. Fluorine in medicinal chemistry. *ChemBioChem* **2004**, *5* (5), 637–643.
- (38) Karaman, M. W.; Herrgard, S.; Treiber, D. K.; Gallant, P.; Atteridge, C. E.; Campbell, B. T.; Chan, K. W.; Ciceri, P.; Davis, M. I.; Edeen, P. T.; Faraoni, R.; Floyd, M.; Hunt, J. P.; Lockhart, D. J.; Milanov, Z. V.; Morrison, M. J.; Pallares, G.; Patel, H. K.; Pritchard, S.; Wodicka, L. M.; Zarrinkar, P. P. A quantitative analysis of kinase inhibitor selectivity. *Nat. Biotechnol.* **2008**, *26* (1), 127–132.
- (39) Pang, I. H.; Wang, W. H.; Clark, A. F. Acute effects of glaucoma medications on rat intraocular pressure. *Exp. Eye Res.* **2005**, *80* (2), 207–214.
- (40) Pang, I. H.; Clark, A. F. Rodent models for glaucoma retinopathy and optic neuropathy. *J. Glaucoma* **2007**, *16* (5), 483–505.